8-2020

Structural Magnetic Resonance Imaging as a Diagnostic Biomarker of HIV-Associated Neurocognitive Disorders (HAND)

Mikki Schantell
University of Nebraska Medical Center

Structural Magnetic Resonance Imaging as a Diagnostic Biomarker of HIV-Associated Neurocognitive Disorders (HAND)

Mikki Schantell[1,2,3]

Epidemiology Concentration

Lorena Baccaglini, PhD, DDS, MS[1], Jianghu (James) Dong, PhD[4,5], Tony W. Wilson, PhD[2,3], & Pamela E. May, PhD[2]

[1]Department of Epidemiology, College of Public Health, UNMC, Omaha, NE 68198-4335, USA

[2]Department of Neurological Sciences, College of Medicine, UNMC, Omaha, NE 68198-8440, USA

[3]Center for Magnetoencephalography, UNMC, Omaha, NE 68198-8422, USA

[4]Department of Biostatistics, College of Public Health, UNMC, Omaha, NE 68198-4335, USA

[5]Division of Nephrology, College of Medicine, UNMC, Omaha, NE 68198-3040, USA

Abstract

Objective: The goal of this study was to do an exploratory analysis to determine if gray matter brain volumes and cortical thickness measures obtained from structural magnetic resonance imaging (sMRI) can discriminate people with HIV-associated neurocognitive disorders (HAND), neurocognitively unimpaired people with HIV (NU PWH), and HIV-negative controls (HIV- controls) using linear discriminant analyses.

Methods: A total of 231 participants, including 110 PWH and 121 HIV- controls, completed a neuropsychological (NP) battery and an sMRI protocol. The bilateral gray matter volumes and cortical thickness brain regions were analyzed using 18 linear discriminant models to assess the discriminability of gray matter volumes and cortical thickness measures separately. The sensitivity, specificity, positive likelihood ratio (LR+), negative likelihood ratio (LR-), and area under the curve (AUC) were computed for each model using the classification results based on the sMRI measures compared to the NP battery.

Results: Of the 110 PWH, 48 were classified as HAND and 62 were classified as NU PWH using the NP battery. The best performing model was the full sample whole brain gray matter volume model with education included, and had a sensitivity of 75.0% (95% CI: 60.4%-86.4%), a specificity of 92.9% (95% CI: 88.2%-96.2%), and an AUC=0.84 (95% CI: 0.76-0.92).

Conclusion: While sMRI measures could aid to inform HAND diagnoses, more rigorous analysis needs to be done before interpreting these results clinically.

Introduction

Despite advances in treatment such as cART, HAND remains prevalent, with about 40% of those living with HIV experiencing neurocognitive impairment (Master & Ances, 2014). However, estimates of the prevalence of HAND range from 18-55% (Heaton et al., 2010; Antinori et al., 2007; Ellis, Langford, & Masliah, 2007; McArthur & Brew, 2010; Robertson et al., 2020). Though the prevalence of HAD – the most severe form of HAND – has decreased since the advent of cART, the prevalence of ANI and MND have remained consistent, ranging from 33-45% and 12-28%, respectively (Tierney et al., 2017).

Background and Literature Review

The Frascati Criteria

Currently, the Frascati criteria (Antinori et al., 2007) are considered the gold standard for diagnosing HAND, and posit three severity classifications: ANI, which requires two of at least five cognitive domains to be at least one standard deviation (SD) below the mean domain score, and no reported impairment in Activities of Daily Living (ADLs); MND, which requires two cognitive domains to be at least one SD below the mean domain score in conjunction with impairment in ADLs; and HAD, which requires two cognitive domains to be at least two SD below the mean domain score along with considerable impairment in ADLs.

Benefits of the Frascati Criteria

The Frascati criteria have been beneficial in operationalizing a diagnostic framework of HAND, particularly for research. These criteria have been associated with many outcomes of clinical significance, such as differences in brain volumes (Masters & Ances, 2014; Becker et al., 2012; Clifford & Ances, 2013; Heaton et al., 2010), blood-based biomarkers (Robertson et al., 2020), and self-reported measures of functional impairment and health indices (Ghandi et al., 2011). These criteria stress

sensitivity over specificity and are therefore useful in detecting neurocognitive impairment before symptom onset (Tierney et al., 2017).

Criticisms of the Frascati Criteria

The HAND classifications have been criticized for being imprecise and susceptible to biases, making it difficult to discriminate between ANI and MND (Clifford & Ances, 2013). The criteria also require substantial clinical judgment to ascertain how much the observed cognitive impairment is due to HIV infection (Antinori et al., 2007; Tierney et al., 2017). Some authors have argued that the criteria are too inclusive and debate the clinical relevance of ANI given its asymptomatic nature, therefore resulting in an overestimation of the prevalence of HAND (Gisslén, Price, & Nilsson, 2011). Additionally, there are other criteria proposed by Gisslén and colleagues (2011) and the Diagnostic and Statistical Manual of Mental Disorders (5th ed.; DSM-5; American Psychiatric Association, 2013), which further complicate the estimation of the prevalence of HAND. Due to the imprecision of these classifications, researchers have strived to discover additional measures, such as cerebrospinal fluid (CSF) markers, blood-based markers, and neuroimaging markers.

Potential Biomarkers of HAND

Previously, biomarkers such as HIV viral load and CD4 counts were associated with cognitive impairment (Clifford & Ances, 2013). However, with improvements in cART, these measures are no longer highly associated with HAND (Clifford & Ances, 2013; Robertson et al., 2020). One study showed positive relationships between blood-based biomarkers such pre-ART interleukin-6 (IL-6) and pre-ART percent CD38+/HLA-DR+(CD8+) levels with HAND severity, though blood-based markers were not entirely reflective of neurocognitive functioning (Robertson et al., 2020).

Researchers have also examined CSF for diagnostic biomarkers of HAND. Several studies have found that increased levels of metalloproteinase (MMP) 1 (MMP-1), MMP-7, tumor necrosis factor

alpha (TNF-α), and granulocyte-macrophage colony-stimulating factor (GM-CSF) in the CSF of individuals with HAD versus those without HAD (Conant et al., 1999; Nottet et al., 1996; Perrella et a., 1992). Additionally, Abassi and colleagues (2017) found inverse relationships between CSF concentrations of S100 calcium-binding protein B (S100B), platelet derived growth factor-AA (PDGF-AA), brain-derived neurotrophic factor (BDNF), and soluble receptor for advanced glycation end products (sRAGE) with the odds of MND or HAD. While CSF biomarkers may be promising, lumbar punctures are invasive and can cause some discomfort. Among potential risks are post-operative headache from spinal fluid leak, bleeding, and infection.

Findings from Neuroimaging Studies of HAND

In addition to blood-based biomarkers and CSF biomarkers, many studies have examined the relationship between regions of interest (ROIs) in sMRI and HAND. Prior to the advent of antiretroviral therapy, PWH showed marked brain atrophy, particularly in total white matter, the basal ganglia, and posterior cortex (Aylward et al., 1993; Heindel et al., 1994). Atrophy signaled advanced HIV infection, though atrophy did not always correspond to cognitive impairment (Stout et al., 1998). Despite improvements in cART, PWH still possess decreased cortical thickness, with substantial cortical thinning in the primary sensory and motor areas, increased ventricle size, and decreased cortical volumes (Becker et al., 2012; Cohen et al., 2010; Jernigan et al., 2011; Masters & Ances, 2014; Ragin et al., 2012; Hassanzadeh-Behbahani, 2020).

Numerous studies have found associations between decreased brain volumes and neuropsychological measures such as poor cognitive or motor performance (Masters & Ances, 2014). Bonnet and colleagues (2013) found those with MND and HAD had decreased gray and white matter volumes. Another study found reduced caudate volume was associated with impaired word generation in those with HAND compared to HIV- controls (Thames et al., 2012).

Other neuroimaging modalities have found functional differences in the brain among HIV- controls, NU PWH, and those with HAND using magnetoencephalography (MEG). One study found that NU PWH and those with HAND had attention and visuo-perceptual deficits when performing a visuospatial discrimination task, displaying increased spontaneous gamma activity at baseline in the bilateral posterior primary visual areas, and decreased oscillatory theta activity when compared to HIV- controls (Wiesman et al., 2018). Similarly, Groff and colleagues (2020) discovered those with HAND demonstrated decreased visual gamma activity with increasing age when completing the same task paradigm. There was an interaction between age and group (HAND, NU PWH, and HIV- controls) in the gamma band in the right parieto-occipital cortices and the right and left prefrontal cortices (Groff et al., 2020).

Another study used the Eriksen flanker task (Eriksen & Eriksen, 1974) and found group differences in flanker interference activity in the theta and alpha ranges originating in the frontal and parietal cortices (Lew et al., 2018). Behaviorally, all studies reported group differences in reaction time and percent accuracy, with participants with HAND displaying greater impairment than HIV- controls and NU PWH (Groff et al., 2020; Lew et al., 2018; Wiesman et al., 2018). Despite these findings, to our knowledge, no studies have published the utility of sMRI and other neuroimaging modalities as biomarkers of HAND.

Neuroimaging as a Biomarker in Alzheimer's Disease

Despite the paucity of literature on sMRI as a biomarker of HAND (Mohamed, Barker, Skolasky, & Sacktor, 2018), several studies in the Alzheimer's disease and mild cognitive impairment (MCI) literature have examined sMRI as a biomarker of Alzheimer's disease and MCI. One study found that patients with MCI have decreased gray matter volume in ROIs as compared to age-matched controls, and a ROC curve analysis showed that gray matter volume loss in the medial temporal lobes (MTL) and posterior cingulate gyrus (PCG) had a discriminative accuracy of 87% (Trivedi et al., 2006). Other studies

assessed ROIs across unimpaired controls, MCI, and AD patients and found AUCs of sMRI between 0.71 and 0.96 (Kim et al., 2017; Schmand, Eikelenboom, & van Gool, 2011).

Objectives

A diagnosis of HAND may require lengthy neuropsychological (NP) testing and self-reported measures of activities of daily living (ADLs) (Antinori et al., 2007; Clifford & Ances, 2013). Many other neurocognitive disorders, such as multiple sclerosis, vascular dementia, normal pressure hydrocephalus, and atypical Parkinsonisms, utilize biomarkers such as structural magnetic resonance imaging (sMRI) in tandem with NP test results to inform diagnoses and assessments of a patient's cognitive impairment level, yet no such biomarkers have been included in the diagnostic criteria for HAND. NP scores have been associated with sMRI findings in HAND (Masters & Ances, 2014), but no studies have assessed whether sMRI can accurately discriminate those with HAND versus those without HAND.

Thus, the primary goal of this study was to assess the sensitivity, specificity, likelihood ratio positive (LR+) and likelihood ratio negative (LR-) of sMRI gray matter volumes and cortical thickness measures as compared to a diagnostic NP battery. We hypothesized that sensitivity and specificity of sMRI gray matter volumes and cortical thickness measures compared to an NP battery would be greater than 50%. To accomplish this, we determined if sMRI gray matter volumes and cortical thickness measures can accurately discriminate people with HAND, NU PWH, and HIV- controls. We hypothesized that there would be differences in gray matter volumes and cortical thickness values measured using sMRI comparing participants with HAND, NU PWH, and HIV- controls. In addition to identifying structural differences, this study evaluated if gray matter volumes and cortical thickness could accurately classify HAND, NU PWH, and HIV- controls. We hypothesized that gray matter volumes and cortical thickness values measured using sMRI would accurately classify HAND, NU PWH, and HIV- controls using linear discriminant analyses.

Data and Methods

Setting and Participants

Participants with HIV were recruited from the University of Nebraska Medical Center HIV Clinic, and HIV- controls were recruited from the University of Nebraska Medical Center's Mind, Brain, Health research registry and through brochures distributed throughout the Omaha area using a convenience sampling method. Because the effects of HIV on aging was of interest, PWH and HIV- controls were considered for the study if they were between the ages of 22 to 72 years. Specific inclusion criteria for HIV+ participants included receiving effective cART measured by attaining an undetectable viral load of less than 50 copies/mL within three months of participating in the study. All controls were confirmed HIV- using the OraQuick *ADVANCE*® Rapid HIV-1/2 Antibody Test at the time of NP testing. All participants were excluded for any neurological or psychiatric conditions other than HAND, history of traumatic brain injury, current substance use disorder, current pregnancy, or ferrous metallic implants that could affect participant safety in the MRI or impede MEG data acquisition.

Standard Protocol Approvals and Participant Consents

The University of Nebraska Medical Center's Institutional Review Board reviewed and approved this protocol. Participants received a written detailed description of the study protocol and a verbal explanation of study procedures. Participants were encouraged to ask questions before written informed consent was obtained. Each participant was given a copy of the signed consent form along with their rights as a research participant.

Study Design

The study utilized a cross-sectional design. There were two visits for the study. The first visit included written informed consent, a standardized demographic and medical history interview, an oral

HIV test for presumed HIV- controls, NP testing, and a peripheral blood draw for PWH to collect current CD4 counts and viral loads. CD4 counts and viral loads were not collected on HIV- controls due to costs and increased invasiveness with little benefit to the participant. The first appointment took one and a half hours to complete. The second visit included a MEG scan and an MRI, which took a total of three hours to complete. Both visits were completed within a maximum of three months of one another.

Neuropsychological Testing

All participants underwent an NP battery designed to assess HAND. The battery tested the following cognitive domains: learning (Hopkins Verbal Learning Test – Revised (HVLT-R) Learning Trials 1-3 (Benedict, Schretlen, Groninger, & Brandt, 1998)), memory (HVLT-R Delayed Recall and Recognition Discriminability Index (Benedict et al., 1998)), executive functioning (Comalli Stroop Test Interference Trial (Comalli, Wapner, & Werner, 1962), semantic verbal fluency (Heaton, Miller, Taylor, & Grant, 2004), phonemic verbal fluency (Heaton et al., 2004), and Trail Making Test Part B (Heaton et al., 2004)), processing speed (Comalli Stroop Test Color Trial (Comalli et al., 1962), Wechsler Adult Intelligence Scale (WAIS-III) Digit Symbol Coding (Wechsler, 1997), and Trail Making Part A (Heaton et al., 2004)), attention (WAIS-III Symbol Search (Wechsler, 1997) and Comalli Stroop Word Trial (Comalli et al., 1962), motor (Grooved Pegboard, Dominant and Non-Dominant Hands (Heaton et al., 2004; Klove, 1963)), and premorbid function (Wide Range Achievement Test 4 (WRAT-4) Word Reading (Wilkinson & Robertson, 2006)). Demographically corrected scores were obtained using published normative data and were computed to z-scores. Domain composite scores were computed by averaging the z-scores of assessments that comprised each respective cognitive domain.

Two examiners were calibrated with administration training videos, had to pass a written NP training test, and were certified upon successful completion of a mock administration that was reviewed by the lead neuropsychologist on the study. HAND classifications were assigned per the Frascati criteria

(Antinori et al., 2007) by the neuropsychologist using the composite domain z-scores corrected for age, sex, race, ethnicity, and years of education along with a modified version of the Lawton and Brody (1969) ADL scale to assess perceived functional impairment.

MRI Data Acquisition

Participants were asked to lie supine on the table with an eight-channel head coil fastened as structural T1-weighted images were collected using a 3D-fast-field echo sequence on a Philips Achieva 3.0T X-Series MRI scanner. The parameters for the 3D-fast-field echo sequence were as follows: TR: 8.09 ms; TE: 3.7 ms; field of view: 24 cm; matrix: 256 × 256; slice thickness: 1 mm with no gap; in-plane resolution: 0.9375 × 0.9375 mm; sense factor: 1.5. One radiologist blinded to group condition examined all anatomical images for incidental findings.

Structural MRI Data Processing of Gray Matter Volume and Cortical Thickness

The T1-weighted anatomical images were segmented into gray matter, white matter, and CSF using the standard voxel-based morphometry (VBM) approach in the computation anatomy toolbox (CAT12 v12.6; Gaser & Dahnke, 2016) in Statistical Parametric Mapping (SPM12) software. The acquired T1-weighted images were noise reduced using a spatially-adaptive non-local means (SANLM) denoising filter (Manjón et al., 2010) and a Markov Random Field (Rajapakse et al., 1997). The images were then bias corrected using an affine registration and a local intensity transformation. Additionally, the images were segmented using an adaptive maximum a posterior (AMAP) technique (Ashburner & Friston, 2005) and partial volume estimation (PVE) with a simplified mixed model with two tissue types or less (Tohka et al., 2004). Finally, the images were normalized to MNI space and smoothed using an 8 mm full width at half maximum (FWHM) Gaussian kernel. Images were also normalized to MNI template space, and the 138 manually annotated cortical and subcortical regions provided by Neuromorphometrics, Inc. (http://neuromorphometrics.com) were applied to determine gray matter volumes within pre-defined

regions of interest. Finally, the resulting VBM images were smoothed using an 8mm FWHM Gaussian kernel.

To assess the cortical thickness, T1 images data were analyzed using additional surface-based morphometry calculations in CAT12 (Gaser and Dahnke, 2016) at a resolution of 1 mm^3. Cortical thickness is estimated using a projection-based thickness approach by reconstructing the central surface in a single step (Dahnke, Yotter, & Gaser, 2013). Once the tissue has been segmented, the white matter (WM) distance is estimated, and the local maxima are projected onto other gray matter voxels using a neighboring relationship described by the WM distance. This method considers partial volume correction, sulcal blurring, and sulcal asymmetries. Spherical harmonics were then used to correct for topological defects (Yotter et al., 2011a), and a common coordinate system reparameterized the cortical surface mesh using an algorithm to reduce distortion (Yotter et al., 2011b). To determine the average cortical thickness of gyral anatomy, we applied the Desikan-Killiany (Desikan et al., 2006) atlas to each participant's surface maps. Finally, the resulting maps were resampled and smoothed using a 15 mm FWHM Gaussian kernel.

Voxel-Based Morphometry and Cortical Thickness Maps

Voxel-based morphometry maps and cortical thickness maps showing *p*-values and effect size in the full sample and the random sample were estimated using analysis of covariance (ANCOVA) models within CAT12 in SPM12. These models assessed HIV status (HIV- controls versus PWH), age, and education and their associations with gray matter volume and cortical thickness. HIV status entered as a categorical variable, and age, education, and intracranial volume entered as continuous covariates. An absolute threshold mask of 0.1 was used, and a false discovery rate (FDR) of 0.05 and k threshold of 200 were used to correct for multiple comparisons in all models.

Random Sampling of NU PWH and HIV- Controls

Random samples of 48 NU PWH and 48 HIV- controls were obtained using the RandStream procedure in MATLAB (MATLAB, 2018) to create group sizes that are equal to the HAND group. The purpose of random sampling was to reduce the effects of unequal group sizes on model discriminability and diagnostic statistics.

Linear Discriminant Analyses of Gray Matter Volume and Cortical Thickness to Classify HAND

Discriminant analyses were used to classify HAND, NU PWH, and HIV- controls over logistic regressions to maximize the differences among the groups based on the obtained functions, and because the main purpose of these analyses was to explore the discriminant ability of gray matter volumes and cortical thickness measures. All explanatory variables of interest were assessed for normality, multicollinearity, and outliers by examining skewness and kurtosis, and using pooled covariance matrices. All bilateral gray matter regions were summed together and corrected for intracranial volume (ICV) to remove the confounding effects of total brain size and to avoid collinearity of bilateral regions. Gray matter found in ventricular, white matter, and cerebellar regions were excluded from the analyses due to their non-normal distributions and missing values. All remaining 56 total bilateral cortical and subcortical gray matter regions corrected for ICV were included as explanatory variables into the linear discriminant analysis with group (HAND, NU PWH, and HIV- control) as the response variable. Education was also included as an explanatory variable to determine if it improved discriminability. A backwards selection linear discriminant analysis was conducted by removing any regions that did not differ between groups at a two-sided α=0.05 to provide the best model fit. Gray matter regions corrected for ICV were then added together into subcortical, frontal, parietal, temporal, occipital, and insular regions (Table 11) and were assessed for discriminability. Again,

education was then added to the gray matter volume regional model to assess if discriminability improved.

The same procedures used for gray matter volumes were used for the cortical thickness measures. All bilateral cortical thickness measures were averaged together to obtain an average cortical thickness per region. A total of 33 average cortical thickness measures were included as explanatory variables along with education, and group (HAND, NU PWH, and HIV- control) as the response variable. Again, a backwards selection linear discriminant analysis was used by removing any regions that did not differ between groups at two-sided α=0.05 to provide the best model fit. The cortical thickness regions were then combined into frontal, parietal, temporal, occipital, and insular regions (Table 11). Education was then added to the model to assess if discriminability of the model improved.

Finally, all linear discriminant analyses were repeated using the random sample to examine if discriminability and diagnostic accuracy of the models changed with equal group sizes.

Sensitivity, Specificity, LR+, LR-, and AUC

Sensitivity, specificity, LR+, LR-, and AUC were calculated using the classification results from the linear discriminant analyses for the whole brain gray matter volume model, the reduced gray matter volume model, the whole brain cortical thickness model, and the reduced cortical thickness model with and without education in the full sample and random sample. We used LR+ and LR- to determine diagnostic accuracy over positive and negative predictive values because they are not affected by the prevalence of HAND, and these metrics are more generalizable to other study populations (Fischer, Bachmann, & Jaeschke, 2003).

Statistical Analyses

Data were analyzed using CAT12 in SPM12 software in addition to SAS software, version 9.4 (SAS Institute Inc., Cary, NC, USA). Demographic variables, gray matter volumes, and cortical thickness measures were assessed using one-way ANOVAs, X^2 tests, and Fisher's exact tests when there were fewer than five expected observations in any category. Independent samples *t*-tests assessed differences in HIV metrics such as years since HIV diagnosis, years on ART, CD4 nadir, and current CD4 counts among NU PWH and HAND. These analyses were completed for both the full sample and the random sample with equal group sizes.

Results

Participants

Of the 254 participants recruited for the study, 121 PWH (68 NU PWH and 53 HAND) and 133 HIV- controls, 231 participants, 110 PWH (62 NU PWH and 48 HAND) and 121 HIV- controls successfully completed the NP battery and the MRI (Figure 1). Participants who were lost to follow-up (n=6), had incomplete MRI data (n=15), or had major incidental findings such as a brain tumor (n=2) were excluded from the analyses. Data were not collected on potentially eligible participants and participants examined for eligibility.

Descriptive Data

The three study groups had comparable demographic characteristics (Table 1). An ANOVA of years of education showed differences between groups, $F(2, 230)=34.7$, $p<0.001$. A post hoc Tukey HSD test revealed that NU PWH had more years of education ($p=0.004$), and HIV- controls had more years of education than both the HAND and NU PWH groups ($p<0.001$).

HIV-associated measures such as years since HIV diagnosis, years on ART, nadir CD4 counts, and current CD4 counts were similar between the NU PWH and HAND groups (Table 1). All participants were virally suppressed (HIV viral load < 50 copies/mL) at the time of the NP testing visit.

Figure 1. Flow Diagram of Participant Exclusions and Final Sample Sizes.

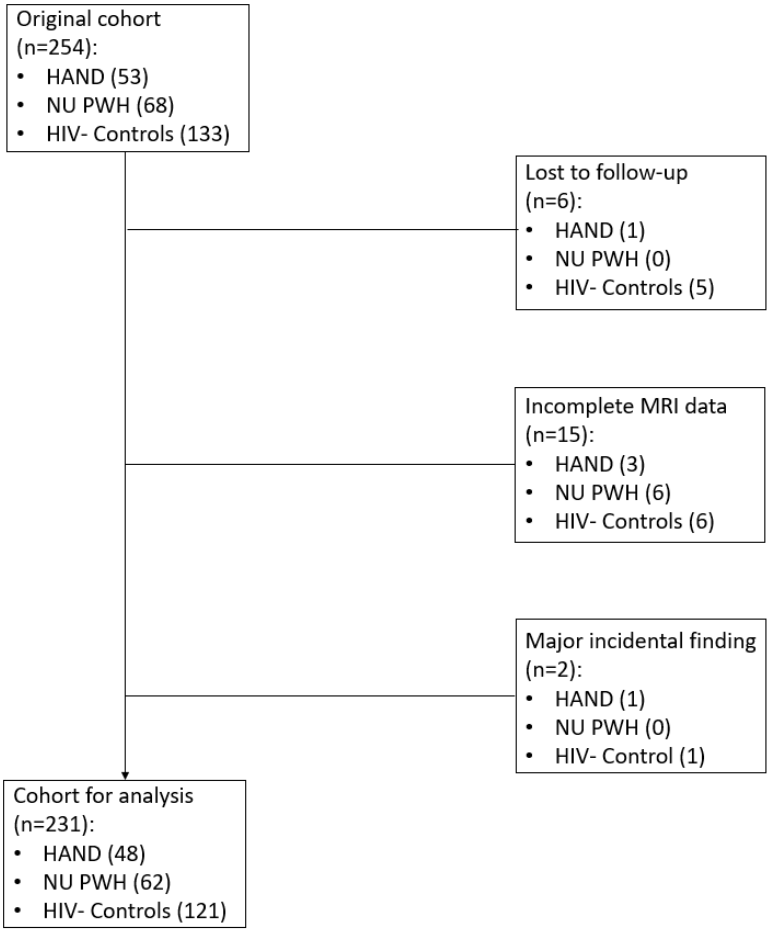

Note. Of the original 254 participants enrolled, 23 participants were excluded for missing or unusable MRI data and major incidental findings that could confound the results of the study.

Neuropsychological Testing Results

Of the 110 PWH who were included in analyses, 48 (43.6%) were classified as having HAND using the NP battery as the gold standard, which is similar to the estimated prevalence of HAND in the United States (Masters & Ances, 2014). Of importance, because we used a convenience sampling procedure,

the prevalence of HAND in this sample should not be heavily interpreted. Among those classified as HAND, 39 (81.3%) were classified as ANI, 5 (10.4%) were classified as MND, and 4 (8.3%) were classified as HAD. Among the HIV- controls, 18 (14.9%) were classified as being cognitively impaired, using the same criteria used to classify ANI. The remaining 103 (85.1%) HIV- controls were NU. Data from missing assessments (e.g., inability to complete Stroop task due to color blindness or Grooved Pegboard task due to a broken wrist) were not considered when classifying impairment.

Groupwise comparisons of each domain showed statistically significant differences in the motor, learning, memory, executive function, processing speed, and attention domains in the full sample and the random sample (p<0.001). Post hoc Tukey HSD tests showed that HAND participants consistently performed worse on all NP domains compared to the other two group (p<0.001), while NU PWH and HIV- controls performed similarly (p>0.05; Table 2).

Table 1. Groupwise Comparisons of Participant Demographics and HIV Metrics

	Full Sample				Random Sample			
Demographics and HIV Metrics	**HAND (n=48)**	**NU PWH (n=62)**	**HIV- Controls (n=121)**	***p***	**HAND (n=48)**	**NU PWH (n=48)**	**HIV- Controls (n=48)**	***p***
Mean age (SD)	46.8 (12.1)	47.7 (12.5)	44.1 (15.4)	0.212	46.8 (12.1)	48.5 (12.0)	43.9 (14.9)	0.215
Sex (frequency, %)[a]								
Females	21 (43.8%)	25 (40.3%)	57 (47.1%)	0.677	21 (43.8%)	19 (39.6%)	22 (45.8%)	0.820
Males	27 (56.2%)	37 (59.7%)	64 (52.9%)		27 (56.2%)	29 (60.4%)	26 (54.2%)	
Race (frequency, %)[b]								
White	26 (54.2%)	45 (72.6%)	82 (67.8%)	0.139	26 (54.2%)	37 (77.1%)	32 (66.7%)	0.136
Black	21 (43.8%)	14 (22.6%)	34 (28.1%)		21 (43.8%)	10 (20.1%)	12 (25.0%)	
Other	1 (1.6%)	5 (8.1%)	5 (4.1%)		1 (1.6%)	1 (2.1%)	4 (8.3%)	
Mean years of education (SD)	13.7 (2.7)	15.2 (2.5)	16.9 (2.2)	<0.001	13.7 (2.7)	15.5 (2.6)	17.4 (2.2)	<0.001
Mean years since HIV diagnosis (SD)[c]	11.7 (7.5)	10.7 (7.2)	-	0.479	11.7 (7.5)	12.1 (7.1)	-	0.797
Mean years on ART (SD)[c]	9.9 (6.7)	8.7 (6.4)	-	0.354	9.9 (6.7)	10.0 (6.2)	-	0.913
Mean CD4 nadir (cells/µL, SD)[c]	222.7 (159.3)	254.4 (166.7)	-	0.317	222.7 (159.3)	230.6 (155.8)	-	0.808
Mean current CD4 count (cells/ µL, SD)[c]	753.1 (409.4)	787.9 (442.2)	-	0.674	753.1 (409.4)	772.2 (462.6)	-	0.831

Note. The full sample included all enrolled participants with complete data. The random sample includes 48 randomly selected NU PWH (neurocognitively unimpaired people with HIV) and HIV- controls to remove the effects of unequal group sizes. HAND – HIV-associated neurocognitive disorder, ART – Antiretroviral therapy, SD – Standard deviation, µL=microliters.

[a] X^2 test.

[b] Fisher's exact test.

[c] Independent samples t test.

Table 2. Groupwise Neuropsychological Test Results by Cognitive Domain

	Full Sample				Random Sample			
Domain z-scores	HAND (n=48)	NU PWH (n=62)	HIV- Controls (n=121)	*p*	HAND (n=48)	NU PWH (n=48)	HIV- Controls (n=48)	*p*
Motor[a]	-1.02 (0.87)	-0.24 (1.02)	-0.33 (0.87)	<0.001	-1.02 (0.87)	-0.21 (1.11)	-0.35 (0.82)	<0.001
Learning[a]	-1.62 (1.10)	-0.18 (0.86)	-0.53 (1.17)	<0.001	-1.62 (1.10)	-0.04 (0.85)	-0.33 (0.96)	<0.001
Memory[a,b]	-1.11 (1.00)	-0.03 (0.67)	-0.29 (0.97)	<0.001	-1.11 (1.00)	0.09 (0.67)	-0.20 (0.94)	<0.001
Executive Function[a]	-0.72 (0.67)	0.08 (0.51)	-0.01 (0.76)	<0.001	-0.72 (0.67)	0.12 (0.52)	-0.03 (0.74)	<0.001
Processing Speed[a]	-0.62 (0.65)	0.24 (0.73)	0.14 (0.73)	<0.001	-0.62 (0.65)	0.31 (0.79)	0.06 (0.77)	<0.001
Attention[a]	-0.98 (0.85)	0.02 (0.58)	0.14 (0.87)	<0.001	-0.98 (0.85)	0.00 (0.61)	0.15 (0.90)	<0.001

Note. Domain scores were calculated by averaging individual assessment z-scores in each respective domain. Analyses of variance (ANOVAs) were computed for each domain by group for the full sample and the random sample. HAND – HIV-associated neurocognitive disorder, NU PWH – Neurocognitively unimpaired people with HIV.

[a]Mean and standard deviation of the domain z-score averaged across assessments.

[b]Eight participants (2 HAND, 3 NU PWH, and 3 HIV- controls) could not complete the task.

Gray Matter Volume and Cortical Thickness Maps

Statistical parametric maps were obtained in SPM12 to assess differences in voxel based morphometry as a measure of gray matter volume among PWH compared to HIV- controls. PWH, including HAND and NU PWH, showed widespread reductions in gray matter volume, after controlling for the independent and interactive effects of age and education and correcting for multiple comparisons using a 0.05 FDR and k=200 threshold (Figure 2). No HIV, age, and education interactions were found. After correcting for multiple comparisons, no differences were found in gray matter volume among those with HAND and NU PWH.

Widespread reductions in cortical thickness were found among HIV- controls and NU PWH and among HIV- controls and those with HAND after adjusting for age and education and correcting for multiple comparisons using a 0.05 FDR and k=200 threshold. Again, no HIV, age, and education interactions were detected, and no cortical thickness clusters were identified among those with HAND and NU PWH.

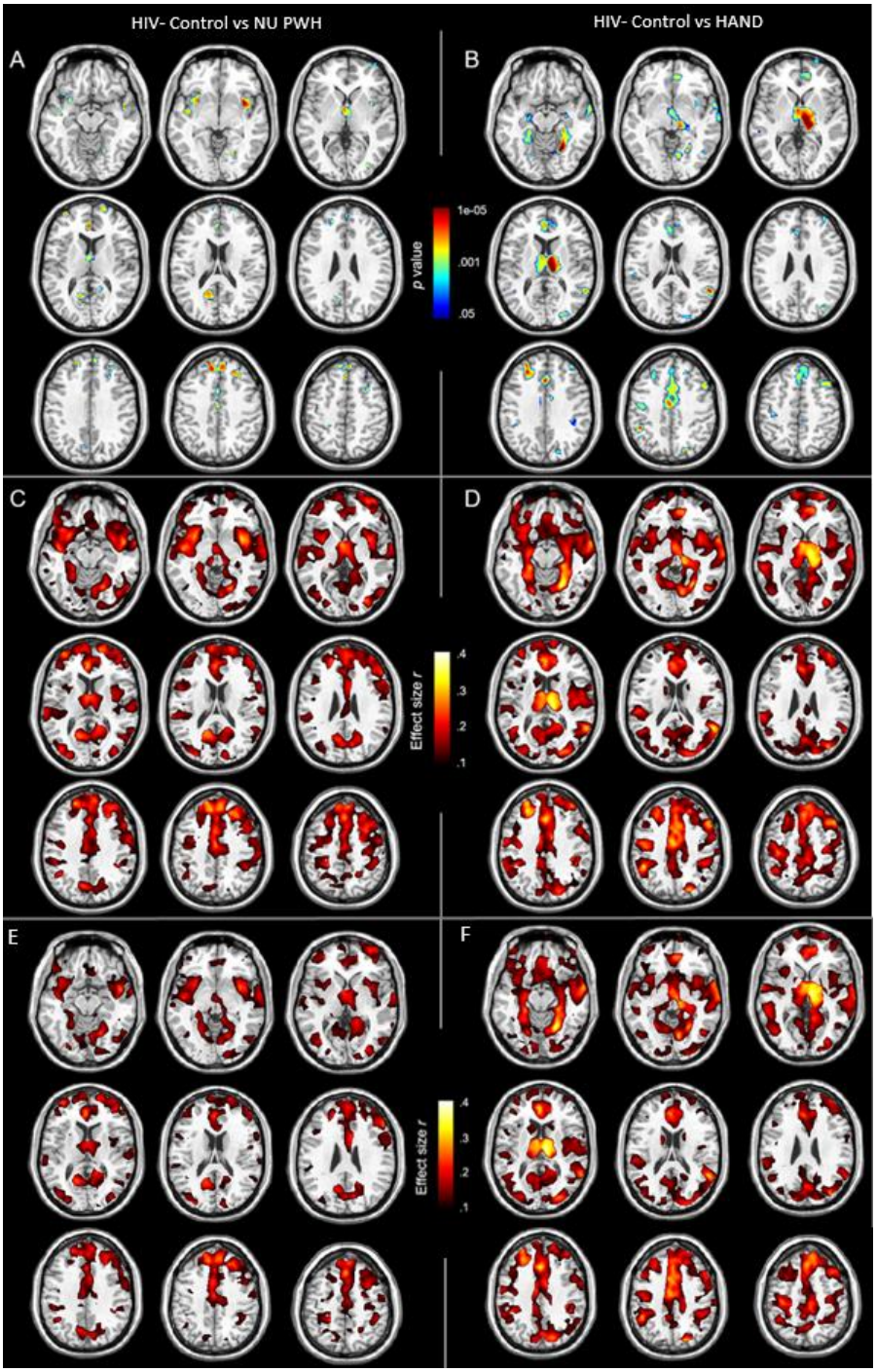

Figure 2. Voxel based morphometry (VBM) maps on the full sample as a proxy of gray matter volume showing groupwise comparisons. (A) HIV- controls (n=121) and NU PWH (n=62) had few clusters showing statistically significant group differences after controlling for the effects of age. (B) Despite reduced power, HIV- controls (n=121) compared to HAND (n=48) showed several significant clusters after controlling for the effects of age. (C) Widespread and relatively small effect sizes (*r*-values) of VMB in HIV- controls compared to NU PWH. (D) Widespread and relatively larger effect sizes of VBM in HIV- controls compared to HAND. (E) Slightly reduced effect sizes in HIV- controls compared to NU PWH after controlling for age and education. (F) Slightly reduced effect sizes in HIV-controls compared to HAND after controlling for age and education. (C,D,E,&F) No clusters survived after correcting for multiple comparisons using a 0.05 FDR and k=200 threshold. No HIV by age and education interactions were found. (A&B) Color bars display *p*-values scaled by -log*(p)*. (C,D,E,&F) Color bars display effect size (*r*-values). The random sample showed similar results, but with reduced significance between groups in the *p*-value maps.

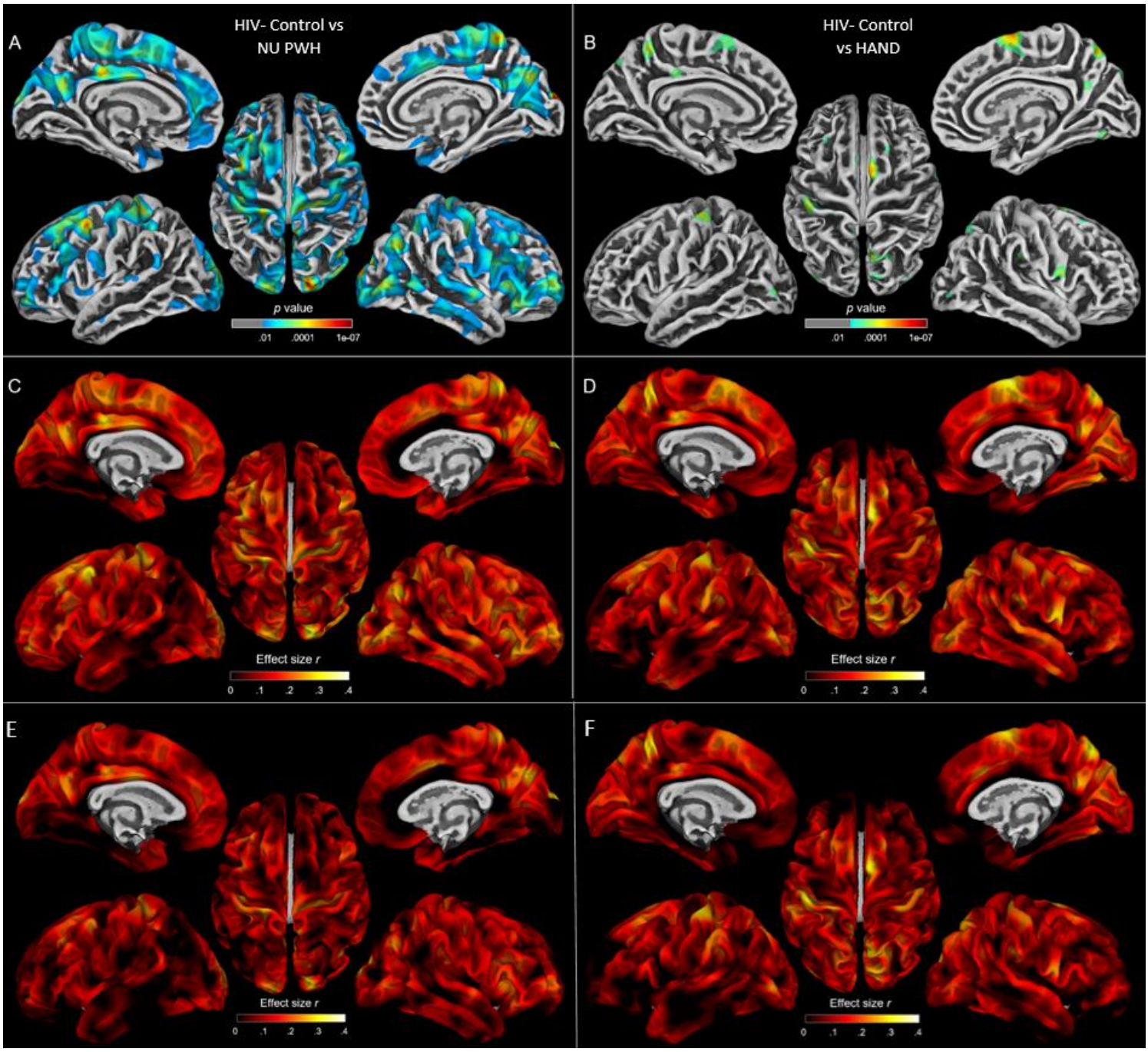

Figure 3. Groupwise comparisons by HAND status on cortical thickness. (A) When comparing HIV- controls (n=121) to NU PWH (n=62), widespread areas showed reductions of cortical thickness after controlling for age. (B) When comparing HIV- controls (n=121) to HAND (n=48), fewer regions showed significant reductions in cortical thickness after correction, potentially due to a reduction in statistical power. (C&D) Effect sizes (*r*-values) of each comparison after controlling for age, which showed a similar pattern and magnitude for the HIV- controls compared to NU PWH in (C) and HIV- controls compared to HAND in (D). (E&F) Effect sizes of each comparison after controlling for age and education, which showed similar results to the comparisons to found in (C&D). No significant clusters were found comparing NU PWH to participants with HAND. The same analyses were done in the random sample with equal group sizes and found the same results, except for reduced significance due to reduced power. The only region that survived in the random sample after correcting for multiple comparisons was the left postcentral gyrus. Color bars display *p*-values scaled by -log(*p*), and corrected with a 0.05 FDR and k=200 threshold. Color bars for the bottom panel display effect size (*r*-values).

Table 3. Groupwise Comparisons of Gray Matter Volumes

Gray Matter Volumes	HAND		NU PWH		HIV- Controls		Test Statistic	
(mm^3)	Mean	SD	Mean	SD	Mean	SD	*F(df)*	*p*
Accumbens	0.000590	0.000085	0.000600	0.000070	0.000603	0.000069	*F*(2,228)=0.85	0.431
Amygdala	0.001323	0.000123	0.001345	0.000129	0.001360	0.000136	*F*(2,228)=2.76	0.065
Caudate	0.004110	0.000549	0.004184	0.000586	0.004184	0.000562	*F*(2,228)=0.27	0.767
Hippocampus	0.004524	0.000452	0.004663	0.000486	0.004683	0.000514	*F*(2,228)=3.12	0.046
Putamen	0.005614	0.000822	0.005522	0.000696	0.005565	0.000705	*F*(2,228)=0.34	0.712
Thalamus	0.006768	0.001124	0.006878	0.000839	0.006896	0.000917	*F*(2,228)=2.52	0.083
Basal Cerebrum and Forebrain	0.000948	0.000116	0.000951	0.000107	0.000955	0.000110	*F*(2,228)=1.94	0.146
Anterior Cingulate Gyrus	0.005939	0.000888	0.006018	0.000757	0.006057	0.000741	*F*(2,228)=6.39	0.002
Anterior Insula	0.006266	0.000775	0.006203	0.000610	0.006214	0.000588	*F*(2,228)=4.12	0.017
Anterior Orbital Gyrus	0.002498	0.000300	0.002496	0.000209	0.002497	0.000233	*F*(2,228)=0.89	0.411
Angular Gyrus	0.012450	0.001642	0.012408	0.001276	0.012463	0.001229	*F*(2,228)=1.76	0.174
Calcarine and Cerebrum	0.004558	0.000613	0.004447	0.000629	0.004494	0.000633	*F*(2,228)=1.19	0.306
Central Operculum	0.005341	0.000621	0.005313	0.000682	0.005314	0.000666	*F*(2,228)=1.89	0.153
Cuneus	0.005409	0.000698	0.005384	0.000588	0.005397	0.000630	*F*(2,228)=6.23	0.002
Entorhinal Area	0.002804	0.000267	0.002900	0.000246	0.002919	0.000252	*F*(2,228)=5.51	0.005
Frontal Operculum	0.002662	0.000346	0.002673	0.000328	0.002677	0.000333	*F*(2,228)=0.70	0.500
Frontal Pole	0.004062	0.000399	0.004054	0.000327	0.004071	0.000358	*F*(2,228)=3.37	0.036
Fusiform Gyrus	0.009958	0.001052	0.010122	0.000922	0.010137	0.000925	*F*(2,228)=6.88	0.001
Gyrus Rectus	0.002374	0.000262	0.002332	0.000214	0.002345	0.000245	*F*(2,228)=2.41	0.092
Inferior Occipital Gyrus	0.007889	0.000982	0.007880	0.000790	0.007872	0.000784	*F*(2,228)=4.90	0.008
Inferior Temporal Gyrus	0.013402	0.001306	0.013355	0.001293	0.013408	0.001308	*F*(2,228)=2.85	0.060
Lingual Gyrus	0.009381	0.001005	0.009343	0.000811	0.009425	0.000817	*F*(2,228)=7.33	0.001
Lateral Orbital Gyrus	0.002686	0.000339	0.002689	0.000299	0.002690	0.000304	*F*(2,228)=5.15	0.006
Middle Cingulate Gyrus	0.005968	0.000774	0.005934	0.000672	0.005970	0.000708	*F*(2,228)=3.80	0.024
Medial Frontal Cerebrum	0.002506	0.000406	0.002509	0.000329	0.002492	0.000342	*F*(2,228)=0.93	0.395
Middle Frontal Gyrus	0.023726	0.002670	0.023721	0.002389	0.023764	0.002434	*F*(2,228)=5.84	0.003
Middle Occipital Gyrus	0.006612	0.000913	0.006633	0.000696	0.006642	0.000721	*F*(2,228)=4.28	0.015
Medial Orbital Gyrus	0.005207	0.000525	0.005168	0.000396	0.005179	0.000438	*F*(2,228)=2.35	0.098
Medial Postcentral Gyrus	0.001254	0.000201	0.001254	0.000182	0.001247	0.000185	*F*(2,228)=1.15	0.320
Medial Precentral Gyrus	0.003271	0.000409	0.003236	0.000432	0.003213	0.000413	*F*(2,228)=3.56	0.030
Superior Medial Frontal Gyrus	0.009046	0.001159	0.009027	0.000941	0.009018	0.000950	*F*(2,228)=4.63	0.011
Middle Temporal Gyrus	0.017973	0.002169	0.017670	0.001869	0.017737	0.001877	*F*(2,228)=2.16	0.117
Occipital Pole	0.004134	0.000622	0.004159	0.000462	0.004159	0.000464	*F*(2,228)=2.12	0.122
Occipital Fusiform Gyrus	0.004197	0.000599	0.004186	0.000488	0.004195	0.000466	*F*(2,228)=3.33	0.038
Inferior Frontal Gyrus	0.004545	0.000618	0.004489	0.000527	0.004467	0.000503	*F*(2,228)=1.04	0.356
Inferior Frontal Orbital Gyrus	0.001921	0.000294	0.001935	0.000259	0.001934	0.000261	*F*(2,228)=1.72	0.182
Posterior Cingulate Gyrus	0.005558	0.000651	0.005608	0.000569	0.005612	0.000588	*F*(2,228)=2.50	0.084
Precuneus	0.013817	0.001594	0.013812	0.001167	0.013837	0.001357	*F*(2,228)=6.33	0.002
Parahippocampal Gyrus	0.003823	0.000313	0.003928	0.000310	0.003948	0.000289	*F*(2,228)=5.91	0.003
Posterior Insula	0.003136	0.000415	0.003100	0.000296	0.003121	0.000293	*F*(2,228)=4.11	0.018
Parietal Operculum	0.002985	0.000445	0.002955	0.000469	0.002961	0.000490	*F*(2,228)=2.94	0.055
Postcentral Gyrus	0.012050	0.001374	0.011999	0.001231	0.012027	0.001224	*F*(2,228)=3.21	0.042
Posterior Orbital Gyrus	0.003495	0.000510	0.003550	0.000403	0.003539	0.000383	*F*(2,228)=7.10	0.001
Planum Polare	0.002670	0.000368	0.002626	0.000257	0.002627	0.000259	*F*(2,228)=5.27	0.006
Precentral Gyrus	0.015855	0.001442	0.015530	0.001478	0.015543	0.001462	*F*(2,228)=4.56	0.011
Planum Temporale	0.002739	0.000357	0.002653	0.000361	0.002640	0.000364	*F*(2,228)=4.10	0.018
Subcallosal Area	0.001544	0.000220	0.001507	0.000176	0.001510	0.000186	*F*(2,228)=2.49	0.085
Superior Frontal Gyrus	0.018072	0.001913	0.017755	0.001485	0.017841	0.001522	*F*(2,228)=9.16	<0.001
Supplementary Motor Cortex	0.006946	0.000802	0.007031	0.000800	0.007013	0.000773	*F*(2,228)=6.32	0.002
Supramarginal Gyrus	0.009906	0.001233	0.009808	0.000977	0.009847	0.000986	*F*(2,228)=2.63	0.074
Superior Occipital Gyrus	0.004310	0.000547	0.004453	0.000521	0.004462	0.000499	*F*(2,228)=2.71	0.069
Superior Parietal Lobule	0.012231	0.001537	0.012063	0.001073	0.012181	0.001129	*F*(2,228)=2.36	0.097
Superior Temporal Gyrus	0.008663	0.001083	0.008540	0.000790	0.008551	0.000775	*F*(2,228)=3.23	0.042
Temporal Pole	0.010602	0.001093	0.010657	0.000944	0.010707	0.000911	*F*(2,228)=2.32	0.100
Inferior Frontal Angular Gyrus	0.004338	0.000596	0.004319	0.000549	0.004295	0.000537	*F*(2,228)=1.50	0.225
Temporal Transverse Gyrus	0.001733	0.000274	0.000600	0.000070	0.001708	0.000226	*F*(2,228)=2.74	0.067

Note. Each region was computed by summing bilateral gray matter regions measured in millimeters cubed (mm^3) and was then divided by intracranial volume (ICV) to reduce the confounding effects of head size. One-way analyses of variance (ANOVAs) were computed for each region by group. HAND – HIV-associated neurocognitive disorder, NU PWH – Neurocognitively unimpaired people with HIV.

Table 4. Groupwise Comparisons of Bilateral Cortical Thickness Regions.

	HAND		NU PWH		HIV- Control		Test Statistic	
Cortical Thickness Regions (mm)	**Mean**	**SD**	**Mean**	**SD**	**Mean**	**SD**	***F(df)***	***p***
Caudal Middle Frontal	2.743	0.179	2.727	0.130	2.806	0.142	$F(2,228)=7.11$	0.001
Cuneus	2.005	0.144	1.999	0.128	2.063	0.135	$F(2,228)=6.00$	0.003
Entorhinal	3.888	0.403	3.875	0.376	4.009	0.350	$F(2,228)=3.51$	0.032
Fusiform	2.693	0.180	2.702	0.157	2.766	0.140	$F(2,228)=5.64$	0.004
Inferior Parietal	2.551	0.143	2.568	0.114	2.612	0.122	$F(2,228)=5.18$	0.006
Inferior Temporal	2.702	0.177	2.718	0.139	2.766	0.138	$F(2,228)=4.10$	0.018
Lateral Occipital	2.189	0.129	2.196	0.105	2.256	0.107	$F(2,228)=9.18$	<0.001
Lingual	2.104	0.165	2.126	0.127	2.165	0.120	$F(2,228)=4.26$	0.015
Medial Orbital Frontal	2.460	0.136	2.456	0.142	2.520	0.131	$F(2,228)=6.15$	0.003
Middle Temporal	2.950	0.196	2.940	0.170	3.019	0.159	$F(2,228)=5.67$	0.004
Parahippocampal	2.577	0.212	2.620	0.171	2.646	0.175	$F(2,228)=2.49$	0.085
Paracentral	2.444	0.187	2.423	0.158	2.526	0.153	$F(2,228)=10.02$	<0.001
Pars Opercularis	2.863	0.182	2.820	0.142	2.909	0.133	$F(2,228)=7.79$	0.001
Pars Orbitalis	2.861	0.215	2.859	0.174	2.932	0.172	$F(2,228)=4.49$	0.012
Pars Triangularis	2.731	0.190	2.686	0.138	2.773	0.143	$F(2,228)=6.78$	0.001
Pericalcarine	1.836	0.164	1.848	0.161	1.925	0.157	$F(2,228)=7.75$	0.001
Postcentral	2.182	0.147	2.183	0.131	2.260	0.132	$F(2,228)=9.37$	<0.001
Posterior Cingulate	2.499	0.141	2.495	0.123	2.557	0.105	$F(2,228)=7.44$	0.001
Precentral	2.534	0.195	2.521	0.168	2.622	0.155	$F(2,228)=9.45$	<0.001
Precuneus	2.496	0.153	2.494	0.125	2.567	0.118	$F(2,228)=9.34$	<0.001
Rostral Anterior Cingulate	2.829	0.214	2.867	0.152	2.904	0.173	$F(2,228)=3.23$	0.041
Rostral Middle Frontal	2.612	0.163	2.587	0.126	2.664	0.127	$F(2,228)=7.43$	0.001
Superior Frontal	2.927	0.178	2.921	0.142	3.002	0.152	$F(2,228)=7.48$	0.001
Superior Parietal	2.295	0.133	2.300	0.121	2.361	0.108	$F(2,228)=8.59$	<0.001
Superior Temporal	2.931	0.197	2.920	0.163	2.999	0.169	$F(2,228)=5.27$	0.006
Supramarginal	2.630	0.141	2.639	0.117	2.696	0.122	$F(2,228)=6.86$	0.001
Frontal Pole	2.793	0.210	2.755	0.192	2.831	0.188	$F(2,228)=3.19$	0.043
Temporal Pole	3.793	0.333	3.765	0.341	3.894	0.334	$F(2,228)=3.64$	0.028
Transverse Temporal	2.512	0.301	2.496	0.228	2.590	0.231	$F(2,228)=3.66$	0.027
Insula	3.517	0.221	3.485	0.162	3.559	0.181	$F(2,228)=3.45$	0.034
Banks of the Superior Temporal Sulcus	2.589	0.172	2.615	0.165	2.643	0.146	$F(2,228)=2.22$	0.111
Caudal Anterior Cingulate	2.567	0.218	2.588	0.177	2.619	0.178	$F(2,228)=1.52$	0.222
Isthmus Cingulate	2.447	0.193	2.446	0.141	2.485	0.152	$F(2,228)=1.72$	0.182

Note. Each region was computed by averaging the thickness of each region bilaterally. Cortical thickness was measured in millimeters (mm). One-way analyses of variance (ANOVAs) were computed for each region by group. HAND – HIV-associated neurocognitive disorder, NU PWH – Neurocognitively unimpaired people with HIV.

Table 5. Groupwise Comparisons of Regional Total Gray Matter Volume

Combined Regions (mm^3)	HAND		NU PWH		HIV- Control		Test Statistic	
	Mean	SD	Mean	SD	Mean	SD	*F(df)*	*p*
Subcortical	0.07585	0.00733	0.07506	0.00812	0.0766	0.0064	*F*(2,228)=0.954	0.386
Frontal	0.14393	0.01030	0.14516	0.01176	0.1372	0.0169	*F*(2,228)=7.776	0.001
Parietal	0.05783	0.00590	0.05776	0.00485	0.0598	0.0046	*F*(2,228)=4.689	0.010
Temporal	0.08682	0.00835	0.08685	0.00673	0.0896	0.0067	*F*(2,228)=4.250	0.015
Occipital	0.03988	0.00442	0.04000	0.00344	0.0416	0.0038	*F*(2,228)=5.313	0.006
Insula	0.00940	0.00115	0.00934	0.00084	0.0097	0.0009	*F*(2,228)=4.587	0.011

Note. Gray matter volume regions were combined by summing the volumes corrected for intracranial volume from each region of the respective combined region, shown in Table 10. Gray matter volume was measured in millimeters cubed (mm^3). One-way analyses of variance (ANOVAs) were computed for each region by group. HAND – HIV-associated neurocognitive disorder, NU PWH – Neurocognitively unimpaired people with HIV.

Table 6. Groupwise Comparisons of Regional Cortical Thickness

Combined Regions (mm)	HAND		NU PWH		HIV- Control		Test Statistic	
	Mean	SD	Mean	SD	Mean	SD	*F(df)*	*p*
Frontal	2.678	0.148	2.666	0.117	2.738	0.118	*F*(2,228)=8.45	<0.001
Parietal	2.299	0.130	2.308	0.113	2.371	0.111	*F*(2,228)=9.70	<0.001
Temporal	2.879	0.178	2.877	0.146	2.954	0.132	*F*(2,228)=7.83	0.001
Occipital	2.099	0.136	2.107	0.108	2.161	0.107	*F*(2,228)=7.47	0.001
Insula	3.517	0.221	3.517	0.221	3.559	0.181	*F*(2,228)=3.45	0.034

Note. Cortical thickness regions were combined by averaging the regional cortical thickness from each region in the respective combined region, shown in Table 10. Cortical thickness was measured in millimeters (millimeters). One-way analyses of variance (ANOVAs) were computed for each region by group. HAND – HIV-associated neurocognitive disorder, NU PWH – Neurocognitively unimpaired people with HIV.

Linear Discriminant Analyses

A total of 18 linear discriminant analyses were conducted to classify those with HAND, NU PWH, and HIV- controls based on gray matter volumes and cortical thickness measures in the brain. The first linear discriminant analysis utilized a whole brain approach using the full sample and all 56 bilateral regions corrected for intracranial volume. The regions (Table 7) with their standardized canonical coefficients returned two discriminant functions that combined accounted for 51.5% of the variance, λ=0.49, p=0.019. The first discriminant function alone, which discriminated HAND from HIV- controls, accounted for 34.6% of the variance in group membership. The second discriminant function, which discriminated HAND from NU PWH, accounted for 25.9% of the variance. Group classification was based on group sizes. The prior probabilities of being classified into each group was as follows: HAND=0.208, NU PWH=0.268, and HIV- control=0.524. The sensitivity was 64.6% (95% CI: 49.5%-77.8%), the specificity was 92.9% (95% CI: 88.2%-96.2%), and the AUC was 0.79 (0.70-0.87; Table 11). Adding education to the model improved the sensitivity to 75% (95% CI: 60.4%-86.4%) and the AUC to 0.84 (95% CI: 0.76-0.92).

While the whole brain gray matter volume model sufficiently discriminated HAND, NU PWH, and HIV- controls, many regions were not sufficiently contributing to the model. The reduced model returned two discriminant functions that accounted for 24.0% of the variance, λ=0.760, p=0.299. The first discriminant function alone accounted for 16.3% of the variance in group membership. The second discriminant function, which discriminated HAND and NU PWH, accounted for 9.2% of the variance. Prior probabilities of being classified into each group were the same as the whole brain gray matter model. The sensitivity was 42.2% (95% CI: 29.9%-55.2%), and the specificity was 87.4% (81.4%-92.0%).

Table 7. Standardized Canonical Coefficients for Each Discriminant Function in the Gray Matter Volume Models

	Full Sample Whole Brain Gray Matter Volume		Full Sample Whole Brain Gray Matter Volume with Education		Full Sample Reduced Gray Matter Volume		Random Sample Whole Brain Gray Matter Volume		Random Sample Whole Brain Gray Matter Volume with Education	
Gray Matter Regions	**Function 1**	**Function 2**	**Function 1**	**Function 2**	**Function 1**	**Function 2**	**Function 1**	**Function 2**	**Function 1**	**Function 2**
Accumbens	0.228	0.301	0.333	0.331	-	-	-0.503	0.339	0.115	0.557
Amygdala	-0.449	-0.022	-0.338	-0.148	-	-	0.695	-0.227	0.500	-0.494
Caudate	0.159	0.327	0.008	0.346	-	-	0.313	0.376	0.319	0.204
Hippocampus	0.547	0.237	0.400	0.367	0.415	-0.295	0.153	0.635	0.173	0.496
Putamen	-0.325	-0.352	-0.271	-0.416	-	-	-0.246	-0.648	-0.647	-0.507
Thalamus	0.390	-0.216	0.450	-0.114	-	-	0.321	0.140	0.507	0.013
Basal Cerebrum and Forebrain	-0.448	0.348	-0.666	0.217	-	-	-0.242	-0.079	-0.669	-0.015
Anterior Cingulate Gyrus	0.306	0.223	0.151	0.246	0.229	-0.89	0.323	0.343	0.237	0.162
Anterior Insula	-0.041	-0.632	0.104	-0.561	-0.527	0.152	0.062	-0.320	0.154	-0.295
Anterior Orbital Gyrus	-0.604	0.114	-0.503	0.003	-	-	0.055	-0.262	0.163	-0.240
Angular Gyrus	-0.112	0.547	-0.311	0.440	-	-	-0.808	0.450	-0.545	0.741
Calcarine and Cerebrum	-0.265	-0.206	-0.150	-0.285	-	-	0.441	-0.413	0.357	-0.545
Central Operculum	-0.279	0.001	-0.135	-0.021	-	-	-0.143	0.349	0.096	0.385
Cuneus	-0.041	-0.527	0.037	-0.497	0.203	0.129	0.207	-0.380	0.162	-0.419
Entorhinal Area	0.387	0.437	0.075	0.566	0.212	-0.470	-0.216	0.623	-0.143	0.637
Frontal Operculum	0.196	0.692	-0.076	0.667	-	-	-0.418	0.047	-0.632	0.186
Frontal Pole	0.160	-0.125	0.151	-0.066	-0.031	-0.042	0.180	0.218	0.138	0.115
Fusiform Gyrus	0.582	0.280	0.291	0.336	0.411	-0.144	-0.086	0.491	-0.019	0.470
Gyrus Rectus	0.226	-0.321	0.353	-0.287	-	-	0.759	-0.225	1.124	-0.463
Inferior Occipital Gyrus	0.189	-0.008	0.103	0.053	0.046	-0.081	-0.736	0.259	-0.650	0.529
Inferior Temporal Gyrus	-0.219	0.392	-0.349	0.380	-	-	-0.067	0.453	-0.053	0.424
Lingual Gyrus	0.531	-0.390	0.617	-0.287	0.394	0.348	0.182	-0.320	0.024	-0.367
Lateral Orbital Gyrus	0.267	0.061	0.301	0.154	-0.083	-0.104	-0.049	0.010	-0.223	0.011
Middle Cingulate Gyrus	-0.411	-0.154	-0.163	-0.262	-0.434	-0.053	0.205	-0.429	0.229	-0.454
Medial Frontal Cerebrum	-0.190	0.461	-0.304	0.417	-	-	-0.819	0.630	-0.843	0.874
Middle Frontal Gyrus	0.971	-0.025	0.707	0.252	0.600	-0.340	0.644	0.371	0.346	0.038
Middle Occipital Gyrus	0.248	-0.425	0.305	-0.285	0.238	-0.060	0.693	-0.448	0.514	-0.685
Medial Orbital Gyrus	-0.346	0.066	-0.296	-0.021	-	-	-0.518	-0.243	-0.799	-0.033
Medial Postcentral Gyrus	-0.063	0.294	-0.153	0.274	-	-	-0.238	0.458	-0.194	0.499
Medial Precentral Gyrus	-0.226	-0.266	-0.011	-0.290	-0.117	0.234	0.178	-0.274	0.128	-0.315
Superior Medial Frontal Gyrus	-0.078	-0.103	-0.051	-0.124	-0.602	-0.103	0.425	-0.065	0.417	-0.226
Middle Temporal Gyrus	-0.622	-0.641	-0.375	-0.893	-	-	-0.226	-1.479	-0.330	-1.211
Occipital Pole	-0.116	0.330	-0.063	0.277	-	-	0.133	0.142	0.408	0.098
Occipital Fusiform Gyrus	-0.309	-0.037	-0.174	-0.057	-0.351	-0.121	-0.175	-0.260	-0.238	-0.163
Inferior Frontal Gyrus	-0.380	0.126	-0.236	0.008	-	-	-0.330	-0.078	-0.208	0.075
Inferior Frontal Orbital Gyrus	-0.133	-0.016	-0.046	-0.066	-	-	0.181	0.094	0.466	0.038
Posterior Cingulate Gyrus	-0.295	0.137	-0.228	0.148	-	-	-0.146	0.141	-0.208	0.175
Precuneus	0.636	0.122	0.360	0.260	0.008	0.025	0.753	0.489	0.672	0.119

Parahippocampal Gyrus	-0.026	0.081	-0.044	0.074	0.127	-0.038	0.018	0.049	0.152	0.049
Posterior Insula	0.123	-0.010	-0.003	-0.054	0.148	0.011	0.040	-0.249	-0.168	-0.254
Parietal Operculum	0.188	0.559	-0.159	0.628	-	-	0.419	0.679	-0.068	0.377
Postcentral Gyrus	0.278	-0.128	0.352	-0.079	0.048	-0.153	-0.276	-0.035	-0.157	0.091
Posterior Orbital Gyrus	0.815	-0.193	0.571	-0.019	0.364	0.195	0.485	0.635	0.688	0.381
Planum Polare	-0.034	-0.169	-0.010	-0.204	-0.144	0.280	0.075	-0.072	0.206	-0.080
Precentral Gyrus	-0.404	-0.660	-0.306	-0.786	-0.718	0.406	0.614	-0.963	0.301	-1.116
Planum Temporale	-0.203	-0.840	0.118	-0.907	-0.248	0.187	-0.170	-0.740	-0.019	-0.563
Subcallosal Area	-0.010	-0.309	0.146	-0.301	-	-	0.074	-0.279	0.049	-0.276
Superior Frontal Gyrus	0.356	-0.296	0.234	-0.183	0.481	0.690	0.599	-0.078	0.244	-0.342
Supplementary Motor Cortex	0.348	0.203	0.361	0.254	0.655	-0.224	-0.988	0.281	-0.408	0.697
Supramarginal Gyrus	0.033	-0.190	0.071	-0.186	-	-	0.544	-0.066	0.527	-0.276
Superior Occipital Gyrus	0.254	0.980	-0.065	0.987	-	-	-0.580	1.153	-0.216	1.274
Superior Parietal Lobule	-0.356	-0.209	-0.061	-0.304	-	-	-0.071	-0.385	0.081	-0.293
Superior Temporal Gyrus	-0.164	0.174	-0.080	0.151	-0.377	0.204	0.108	0.262	0.019	0.177
Temporal Pole	0.204	-0.087	0.114	-0.017	-	-	0.078	0.019	-0.258	-0.048
Inferior Frontal Angular Gyrus	-0.415	0.150	-0.465	0.061	-	-	-0.578	-0.078	-0.536	0.167
Temporal Transverse Gyrus	-0.199	0.199	-0.148	0.170	-	-	-0.533	-0.310	-0.363	-0.042
Education	-	-	0.782	-0.070	-	-	-	-	0.911	0.091

Note. The standardized canonical coefficients for the full sample were computed from groups sizes (HAND=48, NU PWH=62, HIV- Control=121). The random sample was computed from equal group sizes (HAND=48, NU PWH=48, HIV-Control=121). Two functions were returned for each model. HAND – HIV-associated neurocognitive disorder, NU PWH – Neurocognitively unimpaired people with HIV.

Another linear discriminant analysis utilized a random sample of 48 participants in the HIV-control group and 48 participants in the NU PWH group to estimate the discriminability when the group sizes are equal using the whole brain gray matter volume approach. The regions (Table 7) with their standardized coefficients returned two discriminant functions that accounted for 70.1% of the variance, λ=0.30, *p*=0.055. The first discriminant function accounted for 47.2% of the variance, and the second discriminant function accounted for 43.3% of the variance. The sensitivity for this model was 60.4% (95% CI: 45.3%-74.2%), the specificity was 82.3% (95% CI: 73.2%-89.3%), and the AUC was 0.84 (95% CI: 0.76-0.92). Including education in the model improved the sensitivity to 72.9% (95% CI: 58.2%-84.7%), the specificity to 90.6% (95% CI: 83.0%-95.6%), and the AUC remain the same at 0.84 (95% CI: 0.76-0.92).

The models using the combined gray matter volume regions (Table 10) poorly discriminated HAND, NU PWH, and HIV- controls. The worst model was the full sample regional gray matter volume model, which did not correctly identify any participants with HAND. The sensitivity was 0.0% (0.0%-7.4%), the specificity was 99.5% (95% CI: 97.0%-100.0%), and the AUC was 0.50 (95% CI: 0.41-0.59). Including education improved the model substantially, with a sensitivity of 47.9% (95% CI: 33.3%-62.8%), a specificity of 89.1% (95% CI: 83.6%-93.2%), and an AUC of 0.69 (95% CI: 0.59-0.78). Interestingly, the random sample models using the combined regions were able to discriminate HAND from NU PWH and HIV- controls to some degree, though these models performed poorly relative to the other models (Table 10).

The cortical thickness models were not able to discriminate HAND from NU PWH and HIV- controls as well as the gray matter volume models. However, the whole brain cortical thickness model using the random samples returned two discriminant functions that accounted for 48.9% of the variance, λ=0.51, p=0.095. The first discriminant function accounted for 23.8% of the variance, and the second discriminant function account for 10.0% of the variance. The sensitivity for the random sample whole brain cortical thickness model was 60.4% (95% CI: 45.3%-74.2%), the specificity was 82.3% (95% CI: 73.2%-89.3%), and the AUC was 0.71 (95% CI: 0.62-0.81). Including education in the model improved the sensitivity of the model to 72.9% (CI 58.2%-74.2%), the specificity to 90.6% (95% CI: 83.0%-95.6%), and the AUC to 0.82 (95% CI: 0.74-0.90). The full sample whole brain cortical thickness models performed worse than the random sample cortical thickness models. Of note, the random sample combined regional cortical thickness model with education included performed relatively well, with a sensitivity of 70.8% (95% CI: 55.9%-83.1%), a sensitivity of 79.2% (95% CI: 69.7%-86.8%), and an AUC of 0.75 (95% CI: 0.66-0.84).

Table 8. Standardized Canonical Coefficients for Each Discriminant Function in the Cortical Thickness Models

	Whole Brain Cortical Thickness		Whole Brain Cortical Thickness with Education		Reduced Cortical Thickness		Random Sample Whole Brain Cortical Thickness		Random Sample Whole Brain Cortical Thickness with Education	
Cortical Thickness Regions	**Function 1**	**Function 2**	**Function 1**	**Function 2**	**Function 1**	**Function 2**	**Function 1**	**Function 2**	**Function 1**	**Function 2**
Caudal Middle Frontal	0.070	-0.149	-0.271	0.173	0.072	-0.169	0.692	-0.135	0.296	0.544
Cuneus	-0.139	-0.539	-0.082	0.142	-0.088	-0.570	-0.314	-0.457	-0.096	0.104
Entorhinal	0.294	-0.079	-0.128	0.332	0.318	-0.089	-0.118	-0.114	-0.357	0.088
Fusiform	-0.090	0.308	0.135	-0.269	-0.145	0.320	-0.356	0.423	-0.297	-0.486
Inferior Parietal	-0.597	0.130	0.014	-0.599	-0.669	0.088	-0.619	0.140	-0.224	-0.511
Inferior Temporal	-0.726	0.182	-0.217	-0.695	-0.742	0.187	-0.303	0.579	0.107	-0.666
Lateral Occipital	0.623	0.322	0.219	0.338	0.651	0.342	1.184	0.045	0.593	0.713
Lingual	-0.540	0.319	-0.092	-0.618	-0.567	0.286	-0.528	0.611	0.104	0.218
Medial Orbital Frontal	0.252	-0.014	0.102	0.195	0.341	-0.001	0.301	-0.022	-0.179	0.109
Middle Temporal	0.308	-.0338	-0.173	0.496	0.184	-0.346	-0.126	-0.224	0.299	-0.097
Parahippocampal	-0.074	0.240	0.154	-0.226	-0.084	0.209	0.201	0.242	-0.005	0.377
Paracentral	0.388	-0.852	-0.304	0.784	0.427	-0.864	0.235	-0.279	-0.225	0.353
Pars Opercularis	0.331	-0.433	0.052	0.493	0.357	-0.442	-0.125	-0.553	0.503	-0.192
Pars Orbitalis	-0.213	0.259	-0.096	-0.348	-0.206	0.240	0.547	0.677	-0.254	0.524
Pars Triangularis	0.047	-0.637	-0.245	0.393	0.045	-0.661	0.028	-0.619	0.625	-0.123
Pericalcarine	0.289	0.518	0.313	-0.045	0.299	0.509	0.502	0.481	0.328	0.236
Postcentral	0.370	0.383	0.52	0.066	0.379	0.391	0.355	-0.077	0.238	0.307
Posterior Cingulate	0.309	0.238	0.129	0.129	0.286	0.195	0.547	0.068	-0.335	0.047
Precentral	0.144	0.375	0.089	-0.046	0.113	0.384	-0.135	-0.084	-0.404	0.555
Precuneus	0.556	-0.127	0.125	0.551	0.489	-0.130	0.022	-0.612	-0.09	0.095
Rostral Anterior Cingulate	0.103	0.318	-0.027	-0.024	0.000	0.312	0.132	0.045	-0.67	0.472
Rostral Middle Frontal	0.372	-0.442	-0.019	0.576	0.316	-0.442	-0.641	-1.116	0.915	-0.109
Superior Frontal	-0.212	0.718	0.456	-0.647	-0.225	0.755	0.944	0.833	0.297	-0.415
Superior Parietal	-0.024	0.529	0.146	-0.282	0.000	0.557	0.086	0.572	0.100	0.097
Superior Temporal	0.141	-0.100	0.268	0.105	0.133	-0.049	0.075	-0.095	0.073	-0.45
Supramarginal	-0.214	0.192	-0.026	-0.296	-0.280	0.199	-0.336	0.247	-0.355	0.084
Frontal Pole	-0.052	-0.326	-0.085	0.113	-0.037	-0.329	-0.378	-0.395	0.264	-0.050
Temporal Pole	0.028	0.049	0.064	-0.026	0.064	0.053	0.237	0.228	-0.239	-0.227
Transverse Temporal	-0.488	-0.196	-0.487	-0.226	-0.506	-0.202	-0.330	0.056	-0.043	-0.390
Insula	-0.050	-0.308	0.022	0.036	-0.028	-0.334	-0.397	0.139	0.104	0.218
Banks of the Superior Temporal Sulcus	-0.329	0.032	0.104	-0.372	-	-	-0.193	0.394	0.196	-0.477
Caudal Anterior Cingulate	-0.112	-0.006	0.075	-0.136	-	-	-0.010	0.124	0.142	-0.134
Isthmus Cingulate	-0.015	-0.169	-0.071	0.074	-	-	-0.124	-0.192	-0.095	0.065
Education	-	-	0.891	-0.186	-	-	-	-	0.832	-0.229

Note. The standardized canonical coefficients for the full sample were computed from groups sizes (HAND=48, NU PWH=62, HIV-Control=121). The random sample was computed from equal group sizes (HAND=48, NU PWH=48, HIV-Control=121). Two functions were returned for each model. HAND – HIV-associated neurocognitive disorder, NU PWH – Neurocogntively unimpaired people with HIV.

Table 9. Standardized Canonical Coefficients for Each Discriminant Function in the Regional Gray Matter Volume and Cortical Thickness Models

Combined Regions	Full Sample Regional Gray Matter Volume		Full Sample Regional Gray Matter Volume with Education		Random Sample Regional Gray Matter Volume		Random Sample Regional Gray Matter Volume with Education		Full Sample Cortical Thickness		Full Sample Cortical Thickness with Education		Random Sample Cortical Thickness		Random Sample Cortical Thickness with Education	
	Function 1	Function 2	Function 1	Function 2	Function 1	Function 2	Function 1	Function 2	Function 1	Function 2	Function 1	Function 2	Function 1	Function 2	Function 1	Function 2
Subcortical	0.240	-0.829	-0.055	-0.084	-0.176	-0.604	-0.092	0.269	-	-	-	-	-	-	-	-
Frontal	0.743	0.246	-0.408	0.669	-0.055	0.805	0.035	-0.571	0.082	1.848	-0.324	1.612	2.150	-1.588	-0.093	2.645
Parietal	-0.212	-0.108	0.271	-0.121	0.983	0.022	0.632	0.632	0.796	-1.617	0.885	-0.996	-0.252	1.799	1.084	-1.110
Temporal	-0.136	0.691	-0.135	0.042	-0.401	0.345	-0.377	-0.461	0.070	-0.219	-0.226	-0.079	-0.838	0.286	-0.592	-0.774
Occipital	-0.223	0.632	0.249	0.133	0.288	0.253	0.308	0.000	0.142	-0.244	0.030	-0.112	-0.115	0.394	-0.079	-0.229
Insula	-0.336	-0.561	0.000	-0.571	0.278	-0.232	-0.116	0.394	-0.096	0.631	-0.126	0.475	-0.35	-0.562	-0.201	-0.098
Education	-	-	0.878	0.475	-	-	0.962	-0.203	-	-	0.919	-0.214	-	-	0.976	-0.220

Note. The standardized canonical coefficients for the full sample were computed from groups sizes (HAND=48, NU PWH=62, HIV- Control=121). The random sample was computed from equal group sizes (HAND=48, NU PWH=48, HIV-Control=121). Two functions were returned for each model. HAND – HIV-associated neurocognitive disorder, NU PWH – Neurocogntively unimpaired people with HIV.

Table 10. Regions Included in the Combined Gray Matter Volume and Cortical Thickness Regions

Combined Regions	Gray Matter Volume Regions	Cortical Thickness Regions
Subcortical	Accumbens, Amygdala, Caudate, Hippocampus, Putamen, Thalamus, Basal Cerebrum and Forebrain	-
Frontal	Anterior Cingulate Gyrus, Anterior Orbital Gyrus, Central Operculum, Frontal Operculum, Frontal Pole, Gyrus Rectus, Lateral Orbital Gyrus, Middle Cingulate Gyrus, Medial Frontal Cerebrum, Middle Frontal Gyrus, Middle Occipital Gyrus, Medial Orbital Gyrus, Medial Precentral Gyrus, Superior Medial Frontal Gyrus, Inferior Frontal Gyrus, Inferior Frontal Orbital Gyrus, Posterior Orbital Gyrus, Precentral Gyrus, Subcallosal Area, Superior Frontal Gyrus, Supplementary Motor Cortex, Inferior Frontal Angular Gyrus	Caudal Middle Frontal, Medial Orbital Frontal, Paracentral, Pars Opercularis, Pars Orbitalis, Pars Triangularis, Precentral, Rostral Anterior Cingulate, Rostral Middle Frontal, Superior Frontal, Frontal Pole, Caudal Anterior Cingulate, Isthmus Cingulate
Parietal	Medial Postcentral Gyrus, Posterior Cingulate Gyrus, Precuneus, Parietal Operculum, Postcentral Gyrus, Supramarginal Gyrus, Superior Parietal Lobule	Inferior Parietal, Pericalcarine, Postcentral, Superior Parietal, Supramarginal
Temporal	Angular Gyrus, Entorhinal Area, Fusiform Gyrus, Inferior Temporal Gyrus, Middle Temporal Gyrus, Parahippocampal Gyrus, Planum Polare, Planum Temporale, Superior Temporal Gyrus, Temporal Pole, Temporal Transverse Gyrus	Entorhinal, Fusiform, Inferior Temporal, Middle Temporal, Parahippocampal, Posterior Cingulate, Precuneus, Superior Temporal, Temporal Pole, Transverse Temporal, Banks of the Superior Temporal Sulcus
Occipital	Calcarine and Cerebrum, Cuneus, Inferior Occipital Gyrus, Lingual Gyrus, Occipital Pole, Occipital Fusiform Gyrus, Superior Occipital Gyrus	Cuneus, Lateral Occipital, Lingual
Insula	Anterior Insula, Posterior Insula	Insula

Note. Combined gray matter regions were computed by summing the total gray matter volume in each respective region corrected for intracranial volume. Combined cortical thickness regions were computed by averaging the respective regions.

Table 11. Sensitivity, Specificity, Positive Likelihood Ratio, Negative Likelihood Ratio, and Area Under the Curve (AUC) of Structural Magnetic Resonance Imaging Compared with Neuropsychological Testing as the Gold Standard.

Model	Sensitivity	95% CI	Specificity	95% CI	LR+	95% CI	LR-	95% CI	AUC	95% CI
Full Sample WB GMV	64.6%	49.5%-77.8%	92.9%	88.2%-96.2%	9.1	5.2-16.0	0.4	0.3-0.6	0.79	0.70-0.87
Full Sample WB GMV + Education	75.0%	60.4%-86.4%	92.9%	88.2%-96.2%	10.6	6.1-18.3	0.3	0.2-0.4	0.84	0.76-0.92
Full Sample Reduced GMV	42.2%	29.9%-55.2%	87.4%	81.4%-92.0%	3.4	2.1-5.5	0.7	0.5-0.8	0.63	0.53-0.72
Full Sample Regional GMV	0.0%	0.0%-7.4%	99.5%	97.0%-100.0%	0.0	0.0-0.0	1.0	1.0-1.0	0.50	0.41-0.59
Full Sample Regional GMV + Education	47.9%	33.3%-62.8%	89.1%	83.6%-93.2%	4.4	2.6-7.3	0.6	0.4-0.8	0.69	0.59-0.78
Random Sample WB GMV	60.4%	45.3%-74.2%	82.3%	73.2%-89.3%	3.4	2.1-5.6	0.5	0.3-0.7	0.84	0.76-0.92
Random Sample WB GMV + Education	72.9%	58.2%-84.7%	90.6%	83.0%-95.6%	7.8	4.1-14.8	0.3	0.2-0.5	0.84	0.76-0.92
Random Sample Regional GMV	41.7%	27.6%-56.8%	70.8%	60.7%-79.7%	1.4	0.9-2.3	0.8	0.6-1.1	0.55	0.45-0.65
Random Sample Regional GMV + Education	70.8%	55.9%-83.1%	79.2%	69.7%-86.8%	3.4	2.2-5.2	0.4	0.2-0.6	0.69	0.60-0.79
Full Sample WB Cortical Thickness	33.3%	20.4%-48.4%	92.4%	87.5%-95.8%	4.4	2.3-8.3	0.7	0.6-0.9	0.63	0.53-0.73
Full Sample WB Cortical Thickness + Education	54.2%	39.2%-68.6%	91.8%	86.8%-95.3%	6.6	3.8-11.5	0.5	0.4-0.7	0.73	0.64-0.82
Full Sample Reduced Cortical Thickness	37.5%	26.4%-49.7%	86.8%	80.5%-91.6%	2.8	1.7-4.7	0.7	0.6-0.9	0.56	0.47-0.66
Full Sample Regional Cortical Thickness	4.2%	0.5%-14.3%	96.2%	92.3%-98.5%	1.1	0.2-5.1	1.0	0.9-1.1	0.50	0.41-0.59
Full Sample Regional Cortical Thickness + Education	50.0%	34.9%-65.1%	88.0%	82.4%-92.3%	4.2	2.6-6.8	0.6	0.4-0.8	0.68	0.59-0.77
Random Sample WB Cortical Thickness	60.4%	45.3%-74.2%	82.3%	73.2%-89.3%	3.4	2.1-5.6	0.5	0.3-0.7	0.71	0.62-0.81
Random Sample WB Cortical Thickness + Education	72.9%	58.2%-84.7%	90.6%	83.0%-95.6%	7.8	4.1-14.8	0.3	0.2-0.5	0.82	0.74-0.90
Random Sample Regional Cortical Thickness	41.7%	27.6%-56.8%	70.8%	60.7%-79.7%	1.4	0.9-2.3	0.8	0.6-1.1	0.56	0.46-0.66
Random Sample Regional Cortical Thickness + Education	70.8%	55.9%-83.1%	79.2%	69.7%-86.8%	3.4	2.2-5.2	0.4	0.2-0.6	0.75	0.66-0.84

Note. Sensitivity, specificity, LR+, LR-, and AUC were computed using the classification results from the linear discriminant analyses. WB – Whole Brain, GMV – Gray Matter Volume, LR+ – Positive Likelihood Ratio, LR- – Negative Likelihood Ratio, CI – Confidence Interval. AUC – Area Under the Curve.

Discussion

Key Results

Though gray matter volumes and cortical thickness measures were able to discriminate HAND, NU PWH, and HIV- controls, these results must be interpreted with caution. Because the current literature is inconsistent in which brain regions are affected by HAND, and HAND is not well-understood as a disorder, this analysis was exploratory in nature. Ultimately, this analysis sought to determine if sMRI measures could potentially be useful to inform HAND diagnoses.

The model that balanced sensitivity and specificity the best was the full sample whole brain gray matter volume model with education included. Despite this model having an AUC=0.84 (95% CI: 0.76-0.92), the sensitivity was 75.0% (95% CI: 60.4%-86.4%) and the specificity was 92.9% (95% CI: 88.2%-96.2%). Though there are concerns of overfitting the model, using a whole brain approach may be more appropriate clinically, and may potentially be less biased. Given the small HAND sample in this study, it is hard to ascertain which regions were important for discriminating HAND from NU PWH and HIV-controls. While our coefficients for some regions may have been small, this could be an artifact of a small sample size. Future analyses should consider using bootstrap and jackknife procedures to help stabilize the obtained coefficients (Dalgleish, 1994).

Interestingly, education improved discriminability in all models. Even though several of the neuropsychological assessments included in the battery were corrected for education, there are some differences in those with HAND, NU PWH, and HIV- controls above and beyond education, though it's not clear why. Decreased education levels have been associated with lower cognitive reserve and decreased gray matter volumes, which could potentially explain these differences (Mungas et al., 2018). In other words, having a higher level of education appears to have a protective effect against further cognitive decline due to changes in the brain. However, controlling for education in the statistical

parametric maps did not appear to change the groupwise comparisons of gray matter volumes and cortical thickness.

The one-way ANOVAs of gray matter volumes revealed reductions in the hippocampus, anterior cingulate gyrus, entorhinal area, fusiform gyrus, the parahippocampal gyrus, posterior orbital gyrus, and the supplementary motor cortex. These regions coincide well with the assessments in the neuropsychological battery, and are largely reflective of the ventral and dorsal attention networks and the memory networks (Majerus et al., 2012). The cortical thickness analyses revealed similar results, showing cortical thinning in those with HAND in the fusiform, inferior parietal, inferior temporal, lateral occipital, lingual, parahippocampal, pericalcarine, rostral anterior cingulate, superior parietal, and supramarginal gyri.

The Frascati criteria have been criticized for overestimating impairment in PWH and are especially notorious for overestimating the prevalence of ANI (Gisslén, Price, & Nilsson, 2011). This could potentially explain why the gray matter volumes and cortical thickness measures had relatively poor sensitivities, but high specificities. In other words, the gray matter volumes and cortical thickness measures may have been correctly classifying HAND, but the Frascati criteria used to define HAND in this sample may have incorrectly identified those with HAND who did not truly have HAND. More analyses should be done with different diagnostic criteria to determine if the sensitivities of the sMRI measures improve when HAND is not overestimated.

While this analysis demonstrated that sMRI measures, specifically gray matter volumes, could be useful in redefining the clinical definitions of HAND, more rigorous analysis needs to be done. Specifically, it's not clear what causes HAND or what exactly HAND is as a disorder. Winston and Spudich (2020) argue for clearer phenotypes of cognitive impairment based on biomarkers and other clinical assessments.

Limitations

This study had some limitations. First, it was a cross-sectional study design because HAND status was determined at the same time the neural data was collected. While this is a great design for determining the prevalence of HAND in our sample and the accuracy of a diagnostic test, we could not determine causality or temporality. Because participants were classified as HAND based on the results of the NP battery in the study, we did not know if the participants diagnosed with HAND truly had HAND, which limited the interpretability of the results.

Ideally, the results from the NP battery and the sMRI would be used in conjunction to inform HAND diagnoses. However, because our groups were defined based on the results of the NP battery, we did not explore the diagnostic accuracy of the sMRI measures and NP results combined.

Though HAND was moderately prevalent with a prevalence of 43.6% in our sample of PWH, we were limited in our analyses due to the HAND sample (n=48), which led to wide and imprecise confidence intervals, though the confidence intervals were narrower with the random sample. This analysis may be more appropriate using data from the CNS HIV Antiretroviral Therapy Effects Research (CHARTER) study (Heaton et al., 2010) or the Multicenter AIDS Cohort Study (MACS) for more statistical power.

Finally, we only examined the Neuromorphometrics and Desikan-Killiany atlases. Additional analyses should examine different atlases to determine which atlases provide better or worse diagnostic accuracy when discriminating HAND.

Generalizability

While this study sought to reduce bias whenever possible, these results may not be entirely generalizable to the entire population. In particular, HIV- controls were recruited using a convenience

sampling method, thereby limiting the generalizability of the results of the study and biasing the estimates derived from the sample. Additionally, PWH recruited for this study had to be virally suppressed, could not be diagnosed with any neurological or psychiatric conditions, and could not have any ferromagnetic implants. In general, the participants in this study are likely healthier than the general population, and the results of the study should be interpreted accordingly. Because of this, there is also a concern of spectrum bias, which is why it is essential to test these methods in other study samples.

Conclusion

Though the results of this study demonstrate some promise in the utility of using sMRI measures such as gray matter volume and cortical thickness to aid in diagnosing HAND, more rigorous analysis must be done utilizing various neuropsychological diagnostic criteria, multiple atlases to define structural regions in the brain, and these methods must be applied in different study samples before the results should be interpreted for clinical use.

Literature

Abassi, M., Morawski, B. M., Nakigozi, G., Nakasujja, N., Kong, X., Meya, D. B., . . . Boulware, D. R. (2017). Cerebrospinal fluid biomarkers and HIV-associated neurocognitive disorders in HIV-infected individuals in Rakai, Uganda. *Journal of NeuroVirology, 23*(3), 369-375. doi:10.1007/s13365-016-0505-9

Alakkas, A., Ellis, R. J., Watson, C. W.-M., Umlauf, A., Heaton, R. K., Letendre, S., . . . for the, C. G. (2019). White matter damage, neuroinflammation, and neuronal integrity in HAND. *Journal of NeuroVirology, 25*(1), 32-41. doi:10.1007/s13365-018-0682-9

Antinori, A., Arendt, G., Becker, J. T., Brew, B. J., Byrd, D. A., Cherner, M., . . . Wojna, V. E. (2007). Updated research nosology for HIV-associated neurocognitive disorders. *Neurology, 69*(18), 1789-1799. doi:10.1212/01.WNL.0000287431.88658.8b

American Psychiatric Association. (2013). Diagnostic and statistical manual of mental disorders (DSM-5®). *American Psychiatric Pub.*

Ashburner, J. & Friston, K.J. (2005). Unified segmentation. Neuroimage *26*, 839–851.

Aylward, E. H., Henderer, J. D., McArthur, J. C., Brettschneider, P. D., Harris, G. J., Barta, P. E., & Pearlson, G. D. (1993). Reduced basal ganglia volume in HIV-1-associated dementia: results from quantitative neuroimaging. *Neurology, 43*(10), 2099-2104. doi:10.1212/wnl.43.10.2099

Becker, J. T., Maruca, V., Kingsley, L. A., Sanders, J. M., Alger, J. R., Barker, P. B., . . . Selnes, O. (2012). Factors affecting brain structure in men with HIV disease in the post-HAART era. *Neuroradiology, 54*(2), 113-121. doi:10.1007/s00234-011-0854-2

Benedict, R., Schretlen, D., Groninger, L., & Brandt, J. (1998). Hopkins Verbal Learning Test-Revised: Normative data and analysis of inter-form and test-retest reliabiilty. *The Clinical Neuropsychologist. 12*: 43-55.

Bonnet, F., Amieva, H., Marquant, F., Bernard, C., Bruyand, M., Dauchy, F. A., . . . Chêne, G. (2013). Cognitive disorders in HIV-infected patients: are they HIV-related? *Aids, 27*(3), 391-400. doi:10.1097/QAD.0b013e32835b1019

Clifford, D. B., & Ances, B. M. (2013). HIV-associated neurocognitive disorder. *The Lancet. Infectious diseases, 13*(11), 976-986. doi:10.1016/S1473-3099(13)70269-X

Cohen, R. A., Harezlak, J., Schifitto, G., Hana, G., Clark, U., Gongvatana, A., . . . Navia, B. (2010). Effects of nadir CD4 count and duration of human immunodeficiency virus infection on brain volumes in the highly active antiretroviral therapy era. *J Neurovirol, 16*(1), 25-32. doi:10.3109/13550280903552420

Comalli, P. E., Wapner, S., & Werner, H. (1962). Interference effects of stroop color-word test in childhood, adulthood, and aging. *Journal of Genetic Psychology: Research and Theory on Human Development, 100*, 47-53.

Conant, K., McArthur, J. C., Griffin, D. E., Sjulson, L., Wahl, L. M., & Irani, D. N. (1999). Cerebrospinal fluid levels of MMP-2, 7, and 9 are elevated in association with human immunodeficiency virus dementia. *Ann Neurol, 46*(3), 391-398. doi:10.1002/1531-8249(199909)46:3<391::aid-ana15>3.0.co;2-0

Dahnke, R., Yotter, R.A., & Gaser, C. (2013). Cortical thickness and central surface estimation. Neuroimage *65*, 336–348.

Dalgleish, L. I. (1994). Discriminant analysis: Statistical inference using the jackknife and bootstrap procedures. *Psychological Bulletin, 116*(3), 498–508. https://doi.org/10.1037/0033-2909.116.3.498

Desikan, R. S., Ségonne, F., Fischl, B., Quinn, B. T., Dickerson, B. C., Blacker, D., Buckner, R. L., Dale, A. M., Maguire, R. P., Hyman, B. T., Albert, M. S., & Killiany, R. J. (2006). An automated labeling system

for subdividing the human cerebral cortex on MRI scans into gyral based regions of interest. NeuroImage, 31(3), 968-980. https://doi.org/10.1016/j.neuroimage.2006.01.021

Ellis, R., Langford, D., & Masliah, E. (2007). HIV and antiretroviral therapy in the brain: neuronal injury and repair. *Nat Rev Neurosci, 8*(1), 33-44. doi:10.1038/nrn2040

Eriksen, B. A., & Eriksen, C. W. (1974). Effects of noise letters upon the identification of a target letter in a nonsearch task. *Perception & Psychophysics, 16*(1), 143-149. doi:10.3758/BF03203267

Fischer, J. E., Bachmann, L. M., & Jaeschke, R. (2003). A readers' guide to the interpretation of diagnostic test properties: clinical example of sepsis. *Intensive care medicine*, *29*(7), 1043–1051. https://doi.org/10.1007/s00134-003-1761-8

Gaser, C. & Dahnke, R. (2016). CAT-a computational anatomy toolbox for the analysis of structural MRI data. *HBM, 2016*, 336-348

Gisslén, M., Price, R. W., & Nilsson, S. (2011). The definition of HIV-associated neurocognitive disorders: are we overestimating the real prevalence? *BMC infectious diseases, 11*, 356-356. doi:10.1186/1471-2334-11-356

Groff, B. R., Wiesman, A. I., Rezich, M. T., O'Neill, J., Robertson, K. R., Fox, H. S., . . . Wilson, T. W. (2020). Age-related visual dynamics in HIV-infected adults with cognitive impairment. *Neurology(R) neuroimmunology & neuroinflammation, 7*(3), e690. doi:10.1212/NXI.0000000000000690

Hassanzadeh-Behbahani, S., Shattuck, K. F., Bronshteyn, M., Dawson, M., Diaz, M., Kumar, P., Moore, D. J., Ellis, R. J., & Jiang, X. (2020). Low CD4 nadir linked to widespread cortical thinning in adults living with HIV. *NeuroImage. Clinical*, *25*, 102155. https://doi.org/10.1016/j.nicl.2019.102155

Heaton, R.K., Miller, W., Taylor, M. J., & Grant, I. (2004). Revised comprehensive norms for an expanded Halstead-Reitan bettery: Demographically adjusted neuropsychological norms for African American and Caucasian adults, professional manual. *Lutz, FL: Psychological Assessment Resources, Inc.*

Heaton, R. K., Clifford, D. B., Franklin, D. R., Woods, S. P., Ake, C., Vaida, F., . . . Grant, I. (2010). HIV-associated neurocognitive disorders persist in the era of potent antiretroviral therapy. *CHARTER Study, 75*(23), 2087-2096. doi:10.1212/WNL.0b013e318200d727

Heindel, W. C., Jernigan, T. L., Archibald, S. L., Achim, C. L., Masliah, E., & Wiley, C. A. (1994). The relationship of quantitative brain magnetic resonance imaging measures to neuropathologic indexes of human immunodeficiency virus infection. *Archives of neurology, 51*(11), 1129-1135. doi:10.1001/archneur.1994.00540230067015

Jack, C. R., Jr, Bennett, D. A., Blennow, K., Carrillo, M. C., Dunn, B., Haeberlein, S. B., Holtzman, D. M., Jagust, W., Jessen, F., Karlawish, J., Liu, E., Molinuevo, J. L., Montine, T., Phelps, C., Rankin, K. P., Rowe, C. C., Scheltens, P., Siemers, E., Snyder, H. M., Sperling, R., … Contributors (2018). NIA-AA Research Framework: Toward a biological definition of Alzheimer's disease. Alzheimer's & dementia: the journal of the Alzheimer's Association, 14(4), 535-562. https://doi.org/10.1016/j.jalz2018.02.018

Jernigan, T. L., Archibald, S. L., Fennema-Notestine, C., Taylor, M. J., Theilmann, R. J., Julaton, M. D., . . . Grant, I. (2011). Clinical factors related to brain structure in HIV: the CHARTER study. *J Neurovirol, 17*(3), 248-257. doi:10.1007/s13365-011-0032-7

Klove, H. (1963). Grooved Pegboard. *Lafayette, IN: Lafayette Instruments.*

Kim, H.-G., Park, S., Rhee, H. Y., Lee, K. M., Ryu, C.-W., Rhee, S. J., . . . Jahng, G.-H. (2017). Quantitative susceptibility mapping to evaluate the early stage of Alzheimer's disease. *NeuroImage: Clinical, 16*, 429-438. doi:https://doi.org/10.1016/j.nicl.2017.08.019

Lawton, M. P., & Brody, E. M. (1969). Assessment of Older People: Self-Maintaining and Instrumental Activities of Daily Living1. *The Gerontologist, 9*(3_Part_1), 179-186. doi:10.1093/geront/9.3_Part_1.179

Lew, B. J., McDermott, T. J., Wiesman, A. I., O'Neill, J., Mills, M. S., Robertson, K. R., . . . Wilson, T. W. (2018). Neural dynamics of selective attention deficits in HIV-associated neurocognitive disorder. *Neurology, 91*(20), e1860-e1869. doi:10.1212/wnl.0000000000006504

Majerus, S., Attout, L., D'Argembeau, A., Degueldre, C., Fias, W., Maquet, P., Martinez Perez, T., Stawarczyk, D., Salmon, E., Van der Linden, M., Phillips, C., & Balteau, E. (2012). Attention supports verbal short-term memory via competition between dorsal and ventral attention networks. *Cerebral cortex (New York, N.Y. : 1991)*, *22*(5), 1086–1097. https://doi.org/10.1093/cercor/bhr174

Manjón, J.V., Coupé, P., Martí-Bonmatí, L., Collins, D.L., & Robles, M. (2010). Adaptive non-local means denoising of MR images with spatially varying noise levels: Spatially Adaptive Nonlocal Denoising. J. Magn. Reson. Imaging *31*, 192–203.

Masters, M.C. & Ances, B.M. (2014). Role of neuroimaging in HIV-associated neurocognitive disorders. *Seminars in Neurology, 34*(1), 89-102. doi:10.1055/s-0034-1372346

MATLAB. (2018). *9.7.0.1190202 (R2019b)*. Natick, Massachusetts. The Mathworks Inc.

McArthur, J. C., & Brew, B. J. (2010). HIV-associated neurocognitive disorders: is there a hidden epidemic? *Aids, 24*(9), 1367-1370. doi:10.1097/QAD.0b013e3283391d56

Mohamed, M., Barker, P. B., Skolasky, R. L., & Sacktor, N. (2018). 7T Brain MRS in HIV Infection: Correlation with Cognitive Impairment and Performance on Neuropsychological Tests. AJNR. American journal of neuroradiology, 39(4), 704–712. https://doi.org/10.3174/ajnr.A5547

Mungas, D., Gavett, B., Fletcher, E., Farias, S. T., DeCarli, C., & Reed, B. (2018). Education amplifies brain atrophy effect on cognitive decline: implications for cognitive reserve. Neurobiology of aging, 68, 142–150. https://doi.org/10.1016/j.neurobiolaging.2018.04.002

Nottet, H. S., Persidsky, Y., Sasseville, V. G., Nukuna, A. N., Bock, P., Zhai, Q. H., . . . Gendelman, H. E. (1996). Mechanisms for the transendothelial migration of HIV-1-infected monocytes into brain. *J Immunol, 156*(3), 1284-1295.

Perrella, O., Guerriero, M., Izzo, E., Soscia, M., & Carrieri, P. B. (1992). Interleukin-6 and granulocyte macrophage-CSF in the cerebrospinal fluid from HIV infected subjects with involvement of the central nervous system. *Arq Neuropsiquiatr, 50*(2), 180-182. doi:10.1590/s0004-282x1992000200008

Ragin, A. B., Du, H., Ochs, R., Wu, Y., Sammet, C. L., Shoukry, A., & Epstein, L. G. (2012). Structural brain alterations can be detected early in HIV infection. *Neurology, 79*(24), 2328-2334. doi:10.1212/WNL.0b013e318278b5b4

Rajapakse, J.C., Giedd, J.N., and Rapoport, J.L. (1997). Statistical approach to segmentation of single-channel cerebral MR images. IEEE Trans. Med. Imaging *16*, 176–186.

Roberson, K., Landay, A, Miyahara, S, Vecchio, A, Masters, MC, Brown, TT, & Taiwo, BO. (2020). Limited correlation between systemic biomarkers and neurocognitive performance before and during HIV treatment. *J Neurovirol, 26*(1), 107-113. doi:10.1007/s13365-019-00795-2

SAS Institute. (2013). The SAS system for Windows. Release 9.4. Cary, NC.: SAS Inst.

Schmand, B., Eikelenboom, P., van Gool, W. A., & Initiative, t. A. s. D. N. (2011). Value of Neuropsychological Tests, Neuroimaging, and Biomarkers for Diagnosing Alzheimer's Disease in Younger and Older Age Cohorts. *Journal of the American Geriatrics Society, 59*(9), 1705-1710. doi:10.1111/j.1532-5415.2011.03539.x

Stout, J. C., Ellis, R. J., Jernigan, T. L., Archibald, S. L., Abramson, I., Wolfson, T., . . . Grant, I. (1998). Progressive cerebral volume loss in human immunodeficiency virus infection: a longitudinal volumetric magnetic resonance imaging study. HIV Neurobehavioral Research Center Group. *Arch Neurol, 55*(2), 161-168. doi:10.1001/archneur.55.2.161

Thames, A. D., Foley, J. M., Wright, M. J., Panos, S. E., Ettenhofer, M., Ramezani, A., . . . Hinkin, C. H. (2012). Basal ganglia structures differentially contribute to verbal fluency: evidence from Human

Immunodeficiency Virus (HIV)-infected adults. *Neuropsychologia, 50*(3), 390-395. doi:10.1016/j.neuropsychologia.2011.12.010

Tierney, S. M., Sheppard, D. P., Kordovski, V. M., Faytell, M. P., Avci, G., & Woods, S. P. (2017). A comparison of the sensitivity, stability, and reliability of three diagnostic schemes for HIV-associated neurocognitive disorders. *Journal of NeuroVirology, 23*(3), 404-421. doi:10.1007/s13365-016-0510-z

Tohka, J., Zijdenbos, A., and Evans, A. (2004). Fast and robust parameter estimation for statistical partial volume models in brain MRI. NeuroImage *23*, 84–97.

Trivedi, M. A., Wichmann, A. K., Torgerson, B. M., Ward, M. A., Schmitz, T. W., Ries, M. L., . . . Johnson, S. C. (2006). Structural MRI discriminates individuals with Mild Cognitive Impairment from age-matched controls: A combined neuropsychological and voxel based morphometry study. *Alzheimer's & Dementia, 2*(4), ALZJJALZ200606001. doi:10.1016/j.jalz.2006.06.001

Wechsler, D. (1997). Wechsler Adult Intelligence Scale -- Third Edition. *San Antonio, TX: Psychological Corporation.*

Wiesman, A. I., O'Neill, J., Mills, M. S., Robertson, K. R., Fox, H. S., Swindells, S., & Wilson, T. W. (2018). Aberrant occipital dynamics differentiate HIV-infected patients with and without cognitive impairment. *Brain : a journal of neurology, 141*(6), 1678-1690. doi:10.1093/brain/awy097

Wilkinson, G. S. & Roberson, G. J. (2006). Wide Range Achievement Test 4 professional manual. *Lutz, FL: Psychological Assessment Resources., Inc.*

Winston, A., & Spudich, S. (2020). Cognitive disorders in people living with HIV. The lancet. HIV, 7(7), e504–e513. https://doi.org/10.1016/S2352-3018(20)30107-7

Yotter, R.A., Dahnke, R., Thompson, P.M., & Gaser, C. (2011a). Topological correction of brain surface meshes using spherical harmonics. Hum. Brain Mapp. *32*, 1109–1124.

Yotter, R.A., Thompson, P.M., & Gaser, C. (2011b). Algorithms to improve the reparameterization of spherical mappings of brain surface meshes. J. Neuroimaging *21*, e134–e147.

Application of Public Health Competencies

Foundational Competency:

Analyze quantitative and qualitative data using biostatistics, informatics, and computer-based programming and software, as appropriate (MPHF3).

Concentration Competencies:

Determine strengths and weaknesses of the scientific literature and synthesize the evidence to inform public health practice (EPIMPH1).

Utilize analytical approaches to describe, summarize, and interpret epidemiologic data (EPIMPH4).

Human Subjects

This project has been approved by the University of Nebraska Medical Center Institutional Review Board. Please see the enclosed letter of approval for IRB # 225-14-EP.